UNIVERSITI PUTRA MALAYSIA

CHARACTERIZATION OF POLY(3,4-ETHYLENEDIOXYTHIOPHENE)-SODIUM CARBOXYMETHYL CELLULOSE THIN FILM AND POTENTIAL SENSING OF HYDROQUINONE USING SURFACE PLASMON RESONANCE SPECTROSCOPY

FARAH JUWAIRIYAH ATIQAH BINTI MOHD SIDEK

CHARACTERIZATION OF POLY(3,4-ETHYLENEDIOXYTHIOPHENE)-SODIUM CARBOXYMETHYL CELLULOSE THIN FILM AND POTENTIAL SENSING OF HYDROQUINONE USING SURFACE PLASMON RESONANCE SPECTROSCOPY

By

FARAH JUWAIRIYAH ATIQAH BINTI MOHD SIDEK

195946

Thesis Submitted to the Department of Physics, Universiti Putra Malaysia, in partial Fulfilment of the Requirements for the Degree of Bachelor of Science in Physics with Education (Honours)

February 2022

DEDICATION

To my beloved parents Mohd Sidek bin Duraman and Siti Kamisah binti Boyon

For their endless love and support

To my precious siblings and family

For their support and make my life filled with happiness

To all my very cheerful friends

For the memories that we had been created together and make my life cheerful

To all my lectures

For helping me in this journey thoroughly and the knowledge given to me

Thank you all

ABSTRACT

CHARACTERIZATION OF POLY(3,4-ETHYLENEDIOXYTHIOPHENE)-SODIUM CARBOXYMETHYL CELLULOSE THIN FILM AND POTENTIAL SENSING OF HYDROQUINONE USING SURFACE PLASMON RESONANCE SPECTROSCOPY

By

FARAH JUWAIRIYAH ATIQAH BINTI MOHD SIDEK

195946

February 2022

Supervisor: Assoc. Prof. Dr. Yap Wing Fen (PhD)

Department: Department of Physics, Faculty of Science

Conducting polymer composites are promising materials for a green technological future and are actively being investigated in a variety of applications, including biosensing. In this study, poly(3,4-ethylenedioxythiophene)-sodium carboxymethyl cellulose (PEDOT-NaCMC) composites thin film has been used and the preparation of the composites has been described. The PEDOT-NaCMC thin film was characterized by using Fourier transform infrared spectroscopy which confirms the presence of functional group of the composites. The UV-Visible spectrometer was used to study the optical properties of the PEDOT-NaCMC thin film where the absorbance peaks can be found between 270 nm to 300 nm with the optical band gap 4.10 eV. Next, the incorporation of the PEDOT-NaCMC thin film with optical based sensor which is surface plasmon resonance displayed a positive result towards the various concentration of hydroquinone (HQ) solution where it can be found that the system can detect the HQ as low as 2 nM with the sensitivity of 0.0251° nM^{-1}. Further characterization on surface morphology and surface roughness of the thin film using atomic force microscopy confirmed

the interaction of HQ with the thin film. Thus, the PEDOT-NaCMC thin film has the potential to detect HQ, implying that PEDOT-NaCMC can be used as promising candidates for sensing applications.

ABSTRAK

CIRI-CIRI FILEM NIPIS POLI(3,4-ETILDIOKSITIOFINA)-NATRIUM KARBOKSIMETIL SELULOSA DAN POTENSINYA UNTUK MENGESAN HIDROKUINON MENGGUNAKAN SPEKTROSKOPI RESONANS PERMUKAAN PLASMON

Oleh

FARAH JUWAIRIYAH ATIQAH BINTI MOHD SIDEK

195946

Februari 2022

Penyelia: Prof. Madya Dr. Yap Wing Fen (PhD)

Fakulti: Jabatan Fizik, Fakulti Sains

Komposit konduktor polimer merupakan bahan yang menjanjikan masa depan yang baik untuk teknologi hijau dan sedang dikaji secara aktif dalam pelbagai aplikasi, termasuklah pengesanan bio. Dalam kajian ini, filem nipis komposit poli(3,4-etildioksitiofina)-natrium karboksimetil selulosa (PEDOT-NaCMC) telah digunakan dan penyediaan komposit juga telah diterangkan. Filem nipis PEDOT-NaCMC telah dicirikan dengan menggunakan spektroskopi transformasi Fourier inframerah (FTIR) yang mengesahkan kehadiran kumpulan berfungsi komposit. Spektrometer UV-Visible pula digunakan untuk mengkaji sifat optik filem nipis PEDOT-NaCMC di mana puncak serapan boleh didapati antara 270 nm hingga 300 nm dengan jurang jalur optik, 4.10 eV. Seterusnya, penggabungan filem nipis PEDOT-NaCMC dengan sensor berasaskan optik iaitu resonans permukaan plasmon menunjukkan hasil yang positif terhadap pelbagai kepekatan larutan hidrokuinon (HQ) di mana didapati system itu dapat mengesan HQ serendah 2 nM dengan sensitiviti 0.0251° nM^{-1}. Pencirian lanjut mengenai morfologi permukaan dan kekasaran permukaan filem nipis menggunakan mikroskop daya atom

mengesahkan interaksi HQ dengan filem nipis. Oleh itu, filem nipis PEDOT-NaCMC adalah berpotensi untuk mengesan HQ, dan menunjukkan bahawa PEDOT-NaCMC boleh digunakan sebagai komposit yang baik untuk aplikasi sensor.

ACKNOWLEDGEMENT

All praises to Allah and His blessing for the completion of this thesis. I thank God for all the opportunities, trials and strength that have been given to me during my journey in completing writing the thesis. I learned and experiencing so many things throughout this journey.

First and foremost, I would like to sincerely thank my supervisor Assoc. Prof. Dr. Yap Wing Fen for his guidance, understanding and help throughout the duration of this study and the preparation of this thesis. His invaluable help of constructive comments and suggestions throughout the experimental and thesis works have contributed to the completion of this research.

My deepest gratitude goes to my beloved parents; Mr. Mohd Sidek bin Duraman and Mrs. Siti Kamisah binti Boyon for raising me and provided me with daily needs as well as to my siblings for showering me with endless love, prayers and encouragement which become the reason for me to never give up.

My appreciation also extends to Dr Alia Sheh Omar and all the postgraduates of AOLab, for helping and guiding me from the start until the end of the research. They taught a lot of things regarding the research, and I learned a lot from them. May Allah bless you and ease your journey.

Last but not least, sincere thanks to my final year project teammates, Nur Izzati, Nur Illya Aizzah, Habibuzzikri and Mohd Faris as well as my good friends Najah Wahida, Aflah Aziz and Nur Afiqah for keep giving the mental and physical support during this journey. Thanks for the friendship and memories. To those who indirectly contributed in this research, your kindness means a lot to me. Thank you very much.

TABLE OF CONTENTS

LIST OF FIGURES

LIST OF TABLES

LIST OF ABBREVIATIONS

AFM	Atomic force microscopy
cm	Centimetre
DW	Deionized water
FTIR	Fourier transform infrared spectroscopy
HQ	Hydroquinone
h	Hour
LOD	Limit of detection
m	Minutes
mL	Milliliter
nm	Nanometer
nM	Nanomolar
rpm	Revolution per minute
sec	Seconds
SPR	Surface plasmon resonance

CHAPTER 1
INTRODUCTION

1.1 Poly(3,4-Ethylenedioxythiophene)

Poly(3,4-ethylenedioxythiophene), also known as PEDOT, is a conducting polymer that recently has received a lot of interest in industrial applications and academic studies because of its good properties such as comparatively high conductivity and exceptional stability in conditions surrounding when compared to other polymers and as well as its ability to be transparent in the visible spectrum (Gueye et al., 2020). Scientists in the laboratory in Germany were the first to synthesize and commercialize it under the trade name Baytron in 1988. In the beginning, it is reported that PEDOT has an insolubility issue. However, the case was subsequently solved using Poly (styrene sulfonic acid) (PSS), a water-soluble polyelectrolyte as a charge-balancing dopant during polymerization to yield PEDOT:PSS (Seekaew et al., 2014). The combination of PEDOT:PSS makes a system a water-soluble polyelectrolyte with high electrical conductivity, good film-forming properties and high visible light transmissivity, and remarkable stability well suited for numerous new applications (Hryniewicz et al., 2018). Meanwhile, with its high biocompatibility, low toxicity, and structural stability, PEDOT:PSS has a wide range of possible uses in medical sciences, including identifying biologically essential molecules (Wen & Xu, 2017). Therefore, PEDOT:PSS as a novel material is used to enhance and improve the reliability and versatility of a sensor to be used in this study.

1.2 Sodium Carboxymethyl Cellulose

Carboxymethyl cellulose (CMC), commonly used as sodium carboxymethyl cellulose (NaCMC), is an ionic ether derivative of cellulose formed by the reaction of alkali cellulose with a sodium monochloroacetic combination (Lin et al., 2013). As an anionic water-soluble

polymer, the NaCMC has captivated the attention of researchers owing to its exceptional properties being higher clarity in the spectral region, good film-forming potential, high water absorption and swelling properties. It is physiologically non-toxic and is compatible with a mucous membrane, bone, and skin (Almasi et al., 2010). It is widely used in drug delivery and a variety of industrial sectors such as paper making, textile printing, mineral processing, cosmetics and also pharmaceutical and food processing industries (Barbucci et al., 2000) because of the material commonly available biopolymer that is non-toxic, bio-degradable and bio-compatible and also has excellent film-forming properties. Moreover, Li et al. (2008) reported that CMC film is very well-known as a very efficient acting as stabilizer. Because of this basis, CMC has been utilized as the most suitable additive to enhance the properties of PEDOT:PSS.

1.3 Hydroquinone

Hydroquinone (HQ) or Benzene-1,4-diol is an aromatic organic compound produced by the reduction of quinone and oxidation of aniline or phenol or by reacting the acetylene and carbon monoxide. HQ comes naturally in the form of glucose ether which also recognized as arbutin, in the leaves and fruits of plants. Uses of HQ include manufacturing cosmetics, coal tar production, paper, dye, pharmaceutical industries, pesticides, and photographic developers (Gad & Pham, 2014). In medicine and chemistry, HQ has been used as skin depigmentation or skin whitening agents to lighten the dark patches of skin and treat hyperpigmentation and melasma. However, the Food and Drug Administration (FDA) confirm that HQ can be safely sold in 2% concentrations. Otherwise, higher concentrations (up to 4%) should be prescribed and used with caution. HQ can be continually released into the environment and soil during the manufacturing production process and then will be absorbed by the organisms in the

environment, which brings harm and adverse effect to people's health and life, for example, headache, nausea, fatigue, collapse, liver damage and muscle twitching.

HQ has white colour in colour, odorless, crystalline solid with extremely low vapor pressure. In alcohol, HQ is highly soluble while moderately soluble in water. The European Union (EU) and The American Environmental Protection Agency (EPA) state that HQ is one of the priority pollutants due to its low biodegradable ability and high toxicity in the environment. Therefore, the determination of HQ using significantly selective and sensitive techniques is essential and urgently needed.

1.4 Surface Plasmon Resonance

The earliest report to use the surface plasmon resonance (SPR) technique for chemical sensing was made by Liedberg et al. (1983). SPR is a sensitive optical technique for evaluating the change of refractive index of very thin layers of material absorbed on a metal. Most of the SPR application used the Kretschmann configuration, where metal film, commonly gold and silver, was placed at the interface of two dielectric media. The SPR phenomena occurs when the delocalized electrons in the metal film interact with some of the incident light energy at a defined angle, reducing the intensity of the reflected light (Pattnaik, 2005).

A monochromatic polarized light hit the region between the glass and air at a specific angle will cause the total internal reflection to occur. The incident light will match with the reflective light and the intensity of the electric field then the evanescent waves are produced. When a metal (e.g., gold) is placed at the interface between the air and glass, the energy from the light will pair with the plasmon on the metal surface and consequently will reduce the intensity of the reflected light, therefore, achieving the resonance at the given wavelength and angle, where SPR is occurring. This will result in a sharp dip in the transmitted output power

in the SPR spectrum (Verma & Gupta, 2015). If the chemical composition of the environment within the metal surface of the plasmon field change, there will be a shift at the angle of the reflected light. Then the change of the magnitude can be found out by measuring the angle of the reflected light by the metal surface (Abdi et al., 2012).

SPR is observed as a simple optical technique for interfacial and surface studies and shows greatly unrealized for investigating biomolecules (Fen et al., 2020). SPR is recognized as one of the best emerging sensors due to its highly sensitive, label-free and real-time detection. Therefore, SPR is used in this study to determine the sensing potential of PEDOT-NaCMC in sensing HQ.

1.5 Problem Statements

Hydroquinone (HQ) has numbers of applications in the industries of cosmetics and medical. HQ often overdosed in bleaching cream for its specific function in fading and reducing the pigmented areas of the skin. In addition, HQ has been banned from cosmetics as it has high potential of causing adverse health effects, including skin diseases and kidney diseases. It can be only accessible through prescription by physicians and dermatologists due to its hazards of long-term treatments. Moreover, some cases reported where certain manufacturers added the HQ to some cosmetics illegally to increase the bleaching effect of the cosmetics (Chao et al., 2015). Therefore, it is crucial to produce an uncomplicated and rapid systematic method to detect the micro-amount of HQ. There are numbers of techniques that have been done in sensing HQ, including chromatography and electrochemical methods. Nonetheless, the other methods usually require a complex and time-consuming sample pre-treatment procedure and involve high-cost instruments and long processing time, causing them to be unsuitable for routine analysis. Therefore, to overcome the circumstances, an alternative surface plasmon

resonance (SPR) sensor will be used in this work because it has a more straightforward and uncomplicated procedure, which can save a lot more time and cost since it allows the label-free and real-time detection as well as involving low-cost instrument compared to other methods (Anas et al., 2019).

Thin film is an essential part of sensing HQ using the SPR method. The thin film can be fabricated to have its sensitivity and selectivity towards the HQ. Anas et al. (2019) stated that some novel material could be incorporated in the development of the SPR sensor to increase the reliability and versatility of the SPR sensor. From previous studies, conducting polymer PEDOT was reported as a novel material with unique properties and behavior such as good electrical conductivity and optical transparency (Gueye et al., 2020). Due to its properties, several attempts have been made on PEDOT based composite materials to detect HQ. By far, the lowest detection limit obtained was 0.05 µM by using the electrochemical sensor (Mohanadas et al., 2019). Hence in this study, an attempt was made on PEDOT-NaCMC composite thin film to improve the sensitivity and selectivity in the detection of HQ. It is reported that NaCMC can improve PEDOT long-term stability (Wen & Xu, 2017). Moreover, there are lack of studies related to the combination of PEDOT-NaCMC especially using SPR. Thus, it is the interest of this studies to investigate the structural and optical properties of PEDOT-NaCMC thin film and study the sensing potential toward the detection of HQ using the SPR technique.

1.6 Research Objectives

The objectives of this research are:

i. To characterize the structural and optical properties of PEDOT-NaCMC thin film.
ii. To investigate the potential sensing of PEDOT-NaCMC thin film for detection of hydroquinone using surface plasmon resonance method.

CHAPTER 2
LITERATURE REVIEW

2.1 Structural and Optical Properties of PEDOT Based Composite Materials

Poly (3,4-ethylene dioxythiophene) (PEDOT) has recently become one of the most researched conducting polymers due to its exceptional and exceptional characteristics, such as structural stabilities and superior physicochemical properties. Recently, PEDOT has been fabricated into various PEDOT based-composite materials and tailored to meet the requirements of a particular application. Therefore, the different type of PEDOT composite-based materials' structural and optical properties is studied to get more understanding about the absorbance, reflectance, and transmittance. It is also to help researchers to determine the morphology, topography, crystallinity, size, and presence of the functional group to gain precise information for the declaration of production of PEDOT based composite material.

Seekaew et al. (2014) presented a method for fabricating and analysing flexible poly (3,4-ethylene dioxythiophene) Poly (styrene sulfonate) (PEDOT:PSS) and graphene–PEDOT:PSS gas sensors for ammonia (NH_3) detection using ink-jet printing. For the structural properties, AFM results show the film surface with graphene inclusion becomes rough with numbers of polygonal shapes nano-protrusions in the range of 50 nm to 1500 nm. The average surface roughness is 27.82 nm. Meanwhile, Fourier transform infrared spectroscopy (FTIR) shows S–phenyl bond peaks in sulfonic acid at 1010 cm^{-1}, 1039 cm^{-1} and 1060 cm^{-1}. There are peaks at 1263 cm^{-1} and 705 cm^{-1}, 858 cm^{-1}, and 946 cm^{-1} corresponding to C–O–C stretching vibration peak and CAS bond in the thiophene ring.

Moreover, peak of the thiophene ring is observed at 1521 cm^{-1} due to the C=C stretching vibrations while the CAO bonding peak for PEDOT:PSS at 1126 cm^{-1} is shifted slightly to 1519 cm^{-1} and 1120 cm^{-1} for graphene–PEDOT:PSS. Graphene–PEDOT:PSS also has an

additional C=O carbonyl stretching peak at 1743 cm^{-1}, suggesting that the hybridized graphene–PEDOT:PSS sensing film was successfully formed. In terms of UV-Visible properties, PSS's UV–Visible absorption spectra display two peaks at 254 nm and 260 nm, which correlate to common aromatic ring absorption bands.

Next, Hebbar et al. (2017) used a solvent casting approach to developed composite films of PVA-PEDOT:PSS filled with generated graphene oxide (GO) and reduced graphene oxide (RGO) nanoparticles. Based on the AFM analysis, the composites' surface morphology of the composites appears to be smoother than that of the pure blend, which might be due to attributed to the filling of voids in the polymer blend. The presence of C–H asymmetric and symmetric stretching was verified by the bands observed at 2925 cm^{-1} and 2857 cm^{-1} in the composites' FTIR results. There is also absorption peak observed at 1746 cm^{-1} and 1739 cm^{-1} (C=O stretching), 1648 cm^{-1} and 1626 cm^{-1} (C=C stretching), 1449 cm^{-1}-1435 cm^{-1} ($–CH_2$ bending), 1394 cm^{-1}-1379 cm^{-1} ($–CH_2$ wagging), and 1260 cm^{-1}-1254 cm^{-1} (–CH wagging) respectively. UV-Visible shows that the wavelength of PVA-PEDOT:PSS blend reaches the absorption peak around 950 nm for the optical properties. The maximum wavelength was detected in the range 210-220 nm due to π-π* transition from the polymer blend's carbonyl group or benzene ring present.

Furthermore, in 2018, Pasha & Khasim fabricated low-cost ethylene glycol (EG)-doped PEDOT:PSS (Poly 3,4-ethylenedioxythiophene: polystyrene sulfonate) organic thin film sensors to detect LPG at room temperature. For the structural properties, the AFM result shows the RMS roughness of the EG-doped PEDOT:PSS thin film increases from 5.2 nm to 24.6 nm, compared to 5.2 nm for pure PEDOT:PSS. FTIR spectrum presented the following revelations where the characteristic peaks observed for pure PEDOT:PSS are 3700 cm^{-1} owing to O–H stretching, 3500 cm^{-1} owing to C–H stretching, and 2900 cm^{-1} owing to C=O stretching. The intrinsic vibration of the O=H group causes the absorption band at 1840 cm^{-1}. For the optical

properties, the UV-Visible analysis reveals high absorption peaks in the ultraviolet range (550 nm to 750 nm) and a significant absorption peak in the near-infrared (NIR) region. The production of π-π conjugations in the polymer backbone causes the characteristic peak shifts toward higher wavelength.

2.2 Structural and Optical Properties of NaCMC Based Composite Materials

Carboxymethylcellulose (CMC) or commonly take place as a sodium salt (NaCMC) is an anionic linear polysaccharide derived from cellulose. It is frequently used in industry and research laboratories owing to its uniqueness and varieties of physical properties such as nontoxic nature, water-soluble ability, and good biocompatibility. Optical properties, including absorbance, reflectance, and transmittance, is vital to provide information regarding its characteristics and compatibility. On the other hand, structural properties are essential to be studied as they may explain the presence or absence of functional group, morphology, topography, and crystallinity. Structural and optical properties of NaCMC based composite material can be characterized by using FTIR spectra, AFM and UV-Visible.

Akar & Altınıs (2012) has conducted a study about the characterization of fumaric acid cross-linked sodium carboxymethylcellulose. The structural properties of the research are determined by FTIR spectroscopy and AFM analysis. FTIR analysis show at 3422 cm^{-1}, there are broad absorption band due to the stretching frequency of the hydroxyl group (–OH) and C−H stretching vibration causing band at 2924 cm^{-1}. The existence of the carboxyl group (–COO) was proven by the existence of another prominent absorption band at 1613 cm^{-1}. The band perceived at 1062 cm^{-1} is owing to >CH−O−CH_2 stretching. The broad features evidence strong hydrogen bonding about 3400 cm^{-1} from the OH group. The stretches of carbonyl create an asymmetrical band with a centre at 1707 cm^{-1}. The C=C stretch is clearly visible at 1630 cm^{-1}

in FA cross-linked NaCMC samples, while the strong absorption band of NaCMC can be found at 1613 cm^{-1} has moved to 1594 cm^{-1}. The characteristic band of C=O vibrations of the esterified carboxylic groups is clearly visible at around 1725 cm^{-1}. This proves the ester linkage existence. Meanwhile, AFM shows the result of surface roughness of material about 2.78 nm.

In 2013, Kundu et al. carried out research blending the silk fibroin films with sodium carboxymethylcellulose to increase the film properties. AFM analysis was used to observe the surface morphology of the films. It is observed that a pristine fibroin film has a comparatively smooth surface texture that turns rough when the NaCMC polymer is added. The RMS roughness values of the composites (2.00-4.5 nm) were observed to be significantly higher than pure fibroin film's RMS roughness values which is 0.26 nm, and the features mean height present on the pure fibroin film was 1.55 nm, whereas the composites films had average mean heights ranging from 17 to 60 nm. Next, FTIR spectroscopy of blended film shows that absorption frequencies to β-sheet form were 1630 cm^{-1}, 1530 cm^{-1}, 1265 cm^{-1} and 700 cm^{-1} for amide I, II, III, and V, respectively. Other than that, random coil form produced absorption frequencies at 1660 cm^{-1}, 1235 cm^{-1} and 650 cm^{-1} for amide I, II, III, and V, respectively. Peaks at 1645 cm^{-1} (amide I), 1540 cm^{-1} (amide II), 1241 cm^{-1} (amide III), and 660 cm^{-1} (amide IV) are found in blends of film A-E with varied ratios (50:50 (A), 60:40 (B), 70:30 (C), 80:20 (D), 90:10 (E), and 100:0 (F) (amide V). The band may then be seen at 1060 cm^{-1} due to >CH–O–CH_2 stretching of the carboxymethylcellulose. At 3290 cm^{-1}, the N–H group vibrations can be observed.

In 2016, Prema and his co-workers reported research on the characterization of CMC stabilized nano silver. For the structural properties, AFM and FTIR spectra were used in the study. AFM show that 5 to 15 nm were the range for CMC stabilized silver nanoparticles size and it have a spherical surface topology. The two-dimensional micrograph also shows that the particles were properly separated, with no accumulation. The FTIR spectra of CMC-Ag

nanoparticles was then obtained at 3845 cm^{-1}, 3743 cm^{-1}, 3365 cm^{-1}, 1627 cm^{-1}, 1414 cm^{-1}, 1321 cm^{-1}, 1024 cm^{-1} and 603 cm^{-1}, respectively. Due to the stretching frequency of the OH group, the centre peak for CMC was roughly at 3328 cm^{-1}, and band at 2914 cm^{-1} was associated to C–H stretching vibration. Furthermore, the coupling of N–H and C–O stretching indicated strong absorption band at 1589 cm^{-1}. The band between 1330 cm^{-1} and 1041 cm^{-1} show the C–O stretching and the stretching vibration of C–O and C–C both caused peaks at 1327 cm^{-1} and 1262 cm^{-1}, respectively. The characteristic of the OH group bending vibration appeared at band of 1064 cm^{-1}. Similarly, the bending vibration of OH group was found at 1024 cm^{-1} and at 1321 cm^{-1} for C–O stretching. For the optical properties, it was observed from the UV-Visible that there was peak at 419 nm.

Furthermore, Luna-Martínez et al. (2011) made a research on optical characterization of ZnS–sodium carboxymethyl cellulose nanocomposite films. When compared to the large ZnS particles, the UV-Visible spectra result shows a strong absorption at 322 nm, which then slightly shifted to a shorter wavelength. Different precursor salts of ZnS were needed to produce the optical band gap energies (E_g) for the nanocomposites, which is 3.79 eV (S2), 3.69 eV (S3), and 3.67 eV (S4). Meanwhile, in 2021, Badry and his co-workers have developed solid polymer electrolytes (SPEs) based on plasticized sodium carboxymethyl cellulose/polyethene oxide (CMC/PEO). UV-Visible was used to observe the optical properties of the materials in the wavelength range 200 nm to 1000 nm. Due to the $\pi \rightarrow \pi^*$ transition, the absorption peak of PEO was approximately at 272 nm. If the CMC is replaced with different amounts or quantities, the absorption peak disappears. This indicates that the absorbance of CMC film is somewhat changed when PEO is added.

2.3 Sensing Properties of PEDOT and NaCMC Composite Based-Material for Detection of Hydroquinone

In recent years, various types of sensors have developed around the world for the detection of hydroquinone (HQ). It is because HQ is important for a variety of biological and industrial processes. In contrast, HQ is a carcinogenic chemical that has the potential to harm the central nervous system. On the other hand, conducting polymers are often utilized to improve the speed, sensitivity, and flexibility of sensors and biosensors. PEDOT's excellent conductivity, electrical and spectrochemical characteristics, low bandgap, electrochromic and antistatic capabilities, and good stability are all grounds for its broad interest. Meanwhile, NaCMC is well-known for water-soluble anionic polysaccharide that has great importance in the industry and our everyday life.

The electrochemical sensor has become the most used sensor among the researcher in detecting HQ using PEDOT based composite material. In 2014, Si and co-workers developed a sensitive and selective method for the simultaneous detection of catechol and HQ on a poly(3,4-ethylene dioxythiophene)/nitrogen-doped (PEDOT/NGE/GCE). The results from the study show that for HQ, the sensor showed a linear response to concentrations ranging from 1 to 10 µM, with a low detection limit of 0.18 µM. Next, Yao et al. (2014) used a PEDOT:PSS–Nafion–SWCNT–COOHs film to conduct another simultaneous electrochemical detection of dihydroxy benzene isomers such as catechol (CC), resorcinol (RC), and hydroquinone (HQ) in the same year. The recorded limit of detection is 0.20 µM and a relatively wide linear range of 0.56-50 µM, while the result also reported an excellent linear correlation coefficient with 0.998.

In 2017, Tian and co-workers used a PEDOT-graphene composite to conduct an electrochemical study to detect hydroquinone, catechol, resorcinol, and nitrite. They observed individual, selective, and simultaneous detection of the four analytes. The linear range for HQ

is the same throughout the three types of detection, and it is different for linear equation as the linear equation value is 0.996, 0.998, 0.991, respectively. However, the limit of detection of HQ is both the same in the individual and simultaneous equation for 0.06 µM and 0.08 µM for selective detection. Next, in 2019, Mohanadas and co-workers fabricated Poly (3,4-ethylenedioxythiophene)/reduced graphene oxide/manganese dioxide for simultaneous detection of hydroquinone and catechol by using electrochemical sensing. The linear range acquired from the study is 0.5 µM to 150 µM, with a detection limit of 0.05 µM. They discovered a good linear relationship with a correlation value of 0.990 based on the data collected. The slope of the equation shows 0.053 $\mu M \mu A^{-1}$ which is used to calculate the sensitivity of PEDOT/rGO/MnO_2 towards HQ.

Meanwhile, it is reported that only one study regarding the sensing properties of NaCMC in detection of HQ was found. Fu et al. (2015) fabricated a polyaniline/carboxymethyl cellulose/cellulose nanofibrous mats (PANI/CMC/cellulose nanofibrous mats) modified with laccase (Lac) as a biosensor substrate material to detect catechol. They reported that Lac/PANI/CMC/cellulose/glassy carbon electrode (GCE) has a linear response range of 0.497 µM to 2.27 µM with a correlation value of 0.9999. The study showed high sensitivity with a 0.374 µM of detection limit.

2.4 Detection of Hydroquinone Using Optical Method

An optical sensor converts light rays into an electronic signal. It also used to measure a physical quantity of light and then converts it into a form that may be read by an integrated measuring device, depending on the type of sensor. Commonly, optical sensors are used for contact-less detection, counting or positioning of parts. In the past decades, optical sensors based on electrochemiluminescence, fluorescence, chemiluminescence, photoelectrochemical,

and colorimetric techniques have been widely used to detect HQ due to the excellent sensitivity of the detection techniques.

Based on the successful combination of horseradish peroxidase (HRP) with water-soluble conjugate fluorescence polymers $PPESO_3$, Huang et al. (2011) developed a sensitive and simple detection system for quantitative analysis of both hydroquinone (HQ) and hydrogen peroxide (H_2O_2). The limit of detection of HRP–H_2O_2–$PPESO_3$ for HQ detection was 0.5 µM, which was better than the previously reported electrochemical sensor of 1.0 µM reported by Kan and co-workers in 2008. By using HRP–H_2O_2–$PPESO_3$ for detection of HQ, it is observed that the linear relationship between I_0/I and HQ concentrations in the range of 1.0 µM to 2.0 mM with a correlation coefficient of 0.996. After few years, Li et al. (2015) reported a novel biosensor based on carbon dots (C-dots) that can detect HQ with high sensitivity (HQ). An excellent linear range of 0.1–50 µM between the value of $(F_0–F)/F_0$ and HQ concentration is obtained. The correlation coefficient observed at 0.999 with a limit of detection of 0.1 µM. Moreover, Liu et al. (2018) further demonstrated novel silicon quantum dots applications as probes for HQ detection by using the fluorescence sensor. The result shows SiQD probe can detect HQ at concentrations ranging from 6 to 100 µM with a detection limit of 2.63 µM, and the correlation coefficient achieved was 0.995. Lastly, graphite phase carbon nitride quantum dots (g-CNQDs) is also applied as probes to detect HQ using the fluorescence method. The detection limit was as low as 0.04 µM, while the linear range was 0.5 to 11.6 µM. Overall, it is the fluorescence sensor with the lowest detection limit. With a correlation value of 0.9951, the fluorescence intensity of g-CNQDs is strongly correlated with the concentration of HQ (Chen et al., 2019).

Photoelectrochemical (PEC) is one of the most famous methods used by researchers to detect HQ. The PEC technique inherits the benefits of the electrochemical techniques, including low-cost, simple instrumentation, and high sensitivity. Furthermore, the detection

limits of the PEC method are frequently lower than those of its electrochemical counterpart. In 2017, Wang and co-workers researched the photoelectrical sensor to detect HQ using gold nanoparticle-modified indium tin oxide glass GNPs/ITO coated thin films. With a detection limit of 0.1 μM and a correlation value of 0.997, the linear range for HQ determination was 0.25 μM to 150 μM. In the following year, Zhang et al. (2019) developed a new photoelectrochemical sensor for HQ detection based on graphene and silicon nanowires coated n-silicon/platinum (Gr-SiNWs-Si/Pt). The sensor shows the result of limit of detection achieved was 0.3 μM with the linear range of 10 μM to 300 μM and obtained the sensitivity of the sensor 0.36 μA/μM. Next, for one consecutive year, there are two studies conducted using photoelectrochemical to detect the HQ. The detection of hydroquinone using iron(iii) tetra carboxyl–phthalocyanine sensitized nano TiO_2 composite as photoelectrochemical hydroquinone sensor obtained the detection limit 0.078 μM with photocurrent response signal linear with the concentration of HQ ranging from 0.2 μM to 78 μM (Liu, 2020). On the other hand, to detect HQ, the additional work proposed by Qian et al. (2020) developed a photoelectrochemical sensor based on $BiPO_4$-graphene quantum dots nanocomposites. The experimental results showed that the proposed PEC sensor had a good linear range in the concentration range of 50 nM to 3 μM, as well as a lower detection limit of 3.4 nM, which was among the lowest among previous PEC sensors.

The chemiluminescence of nanomaterial systems has received a lot of interest in recent years as a way to increase sensitivity and stability, owing to the high surface area and unique structure of nanomaterials. There has been little research reported using the chemiluminescence method. First, using a luminol-hydrogen peroxide system catalysed by Jacobsen's catalyst, Wang et al. reported an ultrasensitive, fast, and new flow injection chemiluminescence (FI-CL) approach to determine hydroquinone (HQ) in 2014. The relative CL intensity was linear, with the concentration of HQ ranging from 0.6 ng/mL to 10 ng/mL and the detection limit of the

sensor is 0.1 ng/mL. In the following year, Chao et al. (2015) has utilized Fe_3O_4 magnetic nanoparticles capped with oleic acid and coated with a polymer whose surface was molecularly imprinted for HQ to serve as the recognition element in a flow injection chemiluminescence analysis for hydroquinone (HQ). The chemiluminescence intensity is linearly related to the concentration of HQ in the range from 2.0×10^{-7} mg mL^{-1} to 1.0×10^{-5} mg mL^{-1}, with a detection limit of 7.9×10^{-8} mg mL^{-1} and correlation coefficient of 0.996. In 2016, (Zhang et al., 2016) and colleagues developed a sensitive and simple chemiluminescence technique to detect hydroquinone based on the hydrogen peroxide–luminol–sulphonate–(salen)manganese(III) complex. The analysis was reported to have a wide linear range of 0.1 to 10 ng mL^{-1} under ideal conditions, with a detection limit of 0.05 ng mL^{-1} for HQ.

Electrochemiluminescence (ECL) has lately been widely used to detect biological, positive ion, and pharmaceutical species. It is because of its well-known low background, as well as its easy setup, high detection sensitivity, and good selectivity. Hydroquinone has been detected using high ECL efficiency, zinc selenide quantum dots (ZnSe QDs), and benzoquinone in recent years, with a limit of detection of 0.34 nM and a linear range of 1.0 nM to 1.0 µM (Mo et al., 2018). Moreover, Wang and co-workers developed an effective molecularly imprinted (MIP) electrochemiluminescence (ECL) sensor with graphitic carbon nitride nanosheets (g-C_3N_4 NSs) in 2020. The ECL intensity is shown to be linearly related to the concentration of HQ in the range of 5 nM to 10,000 nM, with an excellent detection limit of 0.2 nM. Last but not least, the most recent optical method in the detection of HQ found was using colorimetric developed by Zhao et al., (2020). The study used colorimetric sensing based on platinum deposited on cadmium sulphide (Pt/CDs), and the limit of detection achieved was 0.165 µM with the linear range of 1.0 µM to 10 µM.

2.5 Detection of Hydroquinone using Surface Plasmon Resonance

Surface plasmon resonance is an optical phenomenon in which monochromatic and p-polarized light fulfilling a resonance condition stimulates a charge-density wave moving at the interface between a metal and dielectric medium (Hashim et al., 2020). SPR sensors are frequently used in a variety of applications because they are sensitive, specific and quantitative, and they do not require the molecules to be labelled (label-free) (Fen et al., 2012). It is crucial to establish a simple and quick analytical method for detecting and monitoring the concentration level of these hazardous chemical because of their toxicity and permanence in the environment. However, to the best of our knowledge there is only one study for the detection of HQ using the SPR method.

Wang et al. (2011) presented a simple method for detecting hydroquinone (HQ) based on the localised surface plasmon resonance light scattering (LSPR-LS) of silver nanoparticles (AgNPs) generated via a modified silver mirror process. Over the range of 0.4-2.5 µM, the LSPR-LS intensity increased linearly, with 70.6 nM limits of determination. The results showed that the current approach for determining HQ is quite sensitive. With a correlation value of 0.9951, there was also a strong linear relationship between the increased intensity of LSPR-LS and the HQ concentrations.

Based on the previous research, it is shown that the surface plasmon resonance technique is low-cost, straightforward, sensitive, and environmentally friendly and high potential for HQ detection. Hence, it is of interest to further explore the potential of SPR in sensing of HQ.

CHAPTER 3
METHODOLOGY

3.1 Reagent and Materials

The poly(3,4-ethylenedioxythiophene)-poly(styrenesulfonate) (PEDOT:PSS) solution, sodium carboxymethyl cellulose (NaCMC), and hydroquinone (HQ) reagent were purchased from Sigma-Aldrich, Germany. Deionized water (DW) was used throughout the experiments. A prism with refractive index, n = 1.7786 at 632.8 nm, and glass coverslips as a substrate (24 mm × 24 mm × 0.1 mm) were purchased from Menzel-Glaser, Braunschweig, Germany.

3.2 Preparation of Hydroquinone Solution

To create the HQ solutions with varying concentrations, the hydroquinone was diluted using the dilution formula $M_1V_1=M_2V_2$. The distilled water was used to produce the 2, 4, 6, 8, and 10 nM concentrations.

3.3 Preparation of PEDOT-NaCMC Thin Film

Firstly, before preparing the PEDOT-NaCMC solution, 10 mg 0.1 wt% NaCMC was diluted in 10 mL of deionized water to produce the NaCMC solution. Then, 1 mL of 1.3 wt% of PEDOT:PSS and 1 mL of NaCMC solution was mixed together and the PEDOT-NaCMC solution was produced. To prepare the thin film, the glass coverslips were first cleaned with acetone to wash away any dirt or fingerprint imprints from the glass surface. Then, using the SC7640 Sputter Coater, one of the glass slips' surfaces was gold-coated for 67 seconds to get a thin gold layer with 50 nm thickness to get an optimal dip in the SPR curve (Hashim et al., 2020). Next, 1 mL of dilute PEDOT-NaCMC solution was added to the gold-coated glass slide and spun for 30 seconds at 3000 revs/min with spin coating to form the PEDOT-NaCMC thin

film (Fauzi et al., 2020). Figure 3.1 shows the preparation process of the PEDOT-NaCMC thin film.

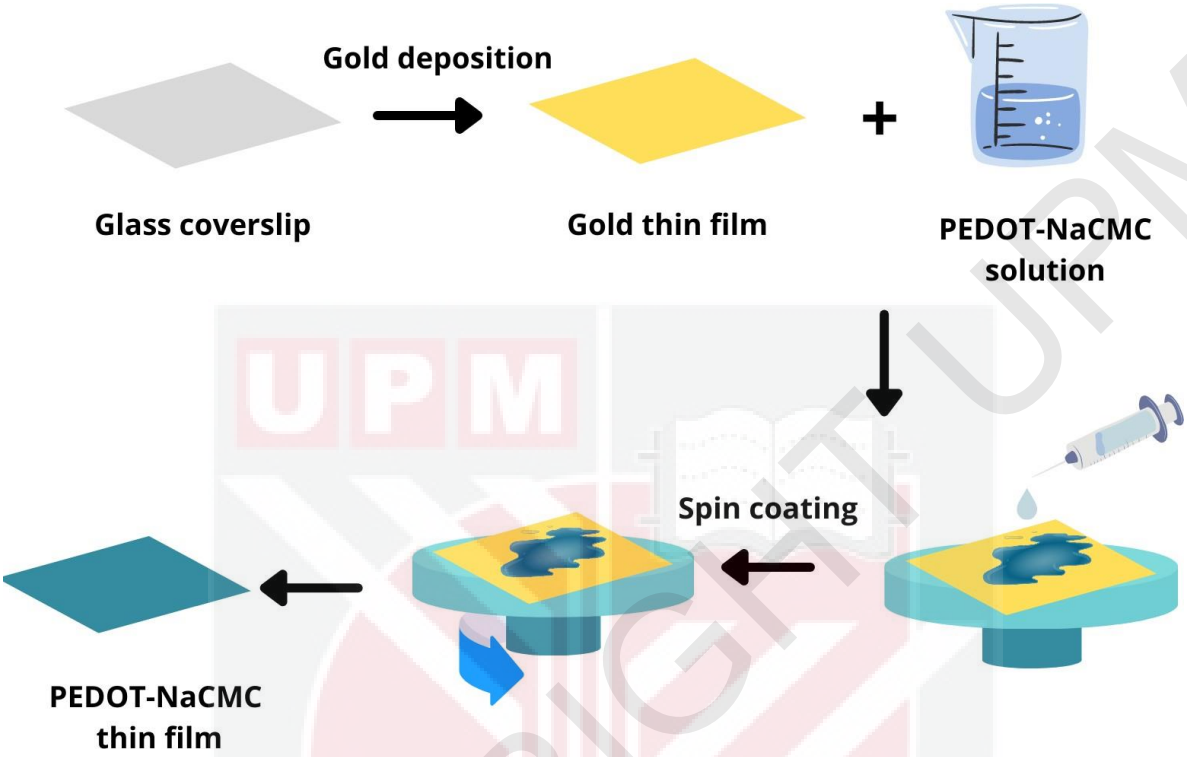

Figure 3.1: Preparation process of the PEDOT-NaCMC thin film.

3.4 Characterization

Fourier transform infrared spectroscopy (FTIR), atomic force microscopy (AFM), and Ultraviolet-Visible spectroscopy (UV-Vis) were used to analyse the structural and optical properties of the thin film PEDOT-NaCMC in this work.

3.4.1 Fourier Transform Infrared Spectroscopy

Fourier transform infrared spectroscopy (FTIR) is used to get the infrared spectrum of transmission or absorption of a solid, liquid, and gas (Song, 2017). FTIR also can identify the presence of organic and inorganic components in a sample. The infrared absorption frequency commonly in the range of 600-4000 cm^{-1} will be used to determine the specific chemical groups present in the sample via spectrum data in automated spectroscopy software. A simple way for this absorption measurement is to focus a monochromatic light beam at a sample and then determine how much of it is being absorbed.

The 'Michelson Interferometer Experimental Setup' laid the basis for FTIR. A source, sample compartment, interferometer, amplifier, detector, A/D converter, and computer are all components of a standard FTIR spectrometer. The interferometer, on the other hand, is made up of a beam splitter, a fixed and moving mirror, and a sensor. Infrared light from the source of light travels along the optical path through a Michelson interferometer in FTIR analysis. When infrared radiation strikes the beam splitter, half of it is refracted and was sent to the fixed mirror, while the other half was sent to the moving mirror. The light is subsequently reflected from the two mirrors to the beam splitter, directed to the detector and source. To retrieve the background spectrum that contains information about absorbed wavelengths by the sample, an interferogram is recorded and transformed to 22 frequency data using the Fourier transform. The working principle of FTIR is shown in Figure 3.2.

In this study, the Perkin-Elmer spectrophotometer (CA, USA) was used to record the FTIR spectrum of PEDOT-sodium carboxymethyl cellulose mixture in the setting of the wavelength range from 400-4000 cm^{-1}.

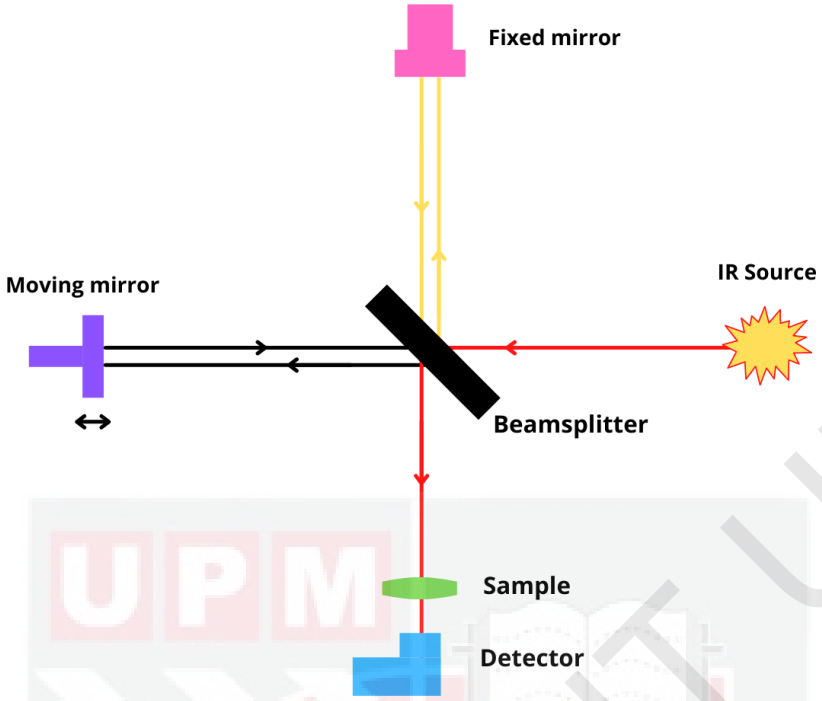

Figure 3.2: Working principle of FTIR.

3.4.2 Atomic Force Microscopy

Atomic force microscopy (AFM) is a powerful imaging method used to examine practically any surface, including polymers, ceramics, composites, glass, and biological materials. Several different forces, including magnetic forces, adhesion strength, and mechanical properties, are measured and localized using AFM. AFM is made up of a sharp tip on a micro-machined silicon probe with a diameter of 10 nm to 20 nm connected to a cantilever (Ray, 2013). The tip is used to image a sample by raster scanning across the surface line by line, regardless of the fact that the technique varies greatly across operating modes (Research, n.d.)

Contact mode and tapping mode are two primary types of operation modes. To protect and prevent both from damage, the tapping mode reduces the contact between the sample

surface and the tip. In the tapping mode, the cantilever is made to vibrate near its resonance frequency, and following that, the tip moves up and down in a sinusoidal pattern. Attractive or repulsive interactions will slow it down when it comes closer to the sample. Rather than the quasistatic deflection, a feedback loop, similar to the contact mode, is utilized to maintain the amplitude of the tapping action constant. Then, the sample's topography will be traced line by line in this method. Tapping mode is the preferable mode because this mode offers some advantages compared to the other modes.

As tapping mode allows high resolution for sensitive samples like thin films, it was used in this work to study the topography and surface of PEDOT-sodium carboxymethyl cellulose using a Q-scope 250 from Quesant Instrument Corporation.

3.3.3 Ultraviolet-Visible Spectroscopy

Ultraviolet-visible Spectroscopy (UV-Vis) is a quantitative method for determining the amount of light absorbed by a chemical compound. This can be determined by comparing the intensity of light passing through a sample to light passing through a blank or reference sample. This method also can be utilized in a variety of sample types, such as glass, liquids, solids, and thin films. Despite the name UV-Vis, the range of the wavenumber that often is used in the near-infrared covers from 190 to 1,100 nm. Using a spectrophotometer and absorption/transmission measurements, researchers may determine the quantity (or concentration) of a specific chemical component. The higher the concentration of a known chemical, the more light it absorbs at one particular wavelength.

As incident light strikes materials, it can absorb, reflect, or transmit. UV-Vis light absorption produces atomic excitation, which shifts molecules from a low-energy ground state to an excited state. Before changing excitation states, an atom must absorb enough radiation to

transfer electrons into higher molecular orbits. Shorter bandgaps are often related to light absorption at shorter wavelengths. As a result, the amount of energy needed for molecules to undergo these transitions varies depending on their electrochemical state.

In this study, the optical characteristics of PEDOT-sodium carboxymethyl cellulose were studied using a UV-Vis-NIR spectrophotometer (UV-3600, Shimadzu) with wavelength settings ranging from 200 nm to 900 nm at room temperature.

3.5 Surface Plasmon Resonance

Surface plasmon resonance (SPR) is a sensitive optical method used to evaluate the change in the index of refraction of thin layers of substance absorbed on a surface of a metal (Rosddi et al., 2021). A polarized beam hits an electrically conducting surface at the interface of two mediums, resulting in SPR. This causes plasmons to occur, which lessen the intensity of reflected light at a specific angle known as the resonance angle, which is proportional to the mass on a surface sensor (Chen et al., 2019)

For this work, SPR optical sensor was used to evaluate the potential of PEDOT-NaCMC thin film to detect hydroquinone. A He-Ne laser, a polarizer, an optical chopper (SR 540), and an optical stage driven by a stepper motor with a resolution of 0.001° (Newport MM 3000) comprise the SPR setup. In the SPR sensor, a p-polarized He-Ne laser with a particular wavelength focus on the prism's varied refractive index. The thin film was placed between the HQ solution and a glass coverslip coated with a chemical connected to one of the prism's sides. An empty cell was built to hold the HQ solution and subsequently connected to the PEDOT-NaCMC surface to store the HQ solution (Anas et al., 2019). Before starting the experiment, HQ solutions of various concentrations were consecutively inserted into the cell, and it was let to be in contact for approximately 2 minutes. A He-Ne laser with a wavelength of 632.8 nm

was used to irradiate the prism, and the prism with the hollow cell was be positioned on a revolving plate to adjust the angle of light emitted. Surface plasmon waves are generated at the interface when incoming light from the He-Ne laser beam travels through the prism and hit the thin film's gold layer. An evanescent wave was formed as a result of a change in the refractive index of the medium near the active layer at a certain angle of incoming light, resulting in the SPR response (Hashim et al., 2020). A photodiode detects the reflected light, which was then processed by the lock-in amplifier (SR 530). Figure 3.3 depicts and summarizes the complete technique and experimental setup of the SPR.

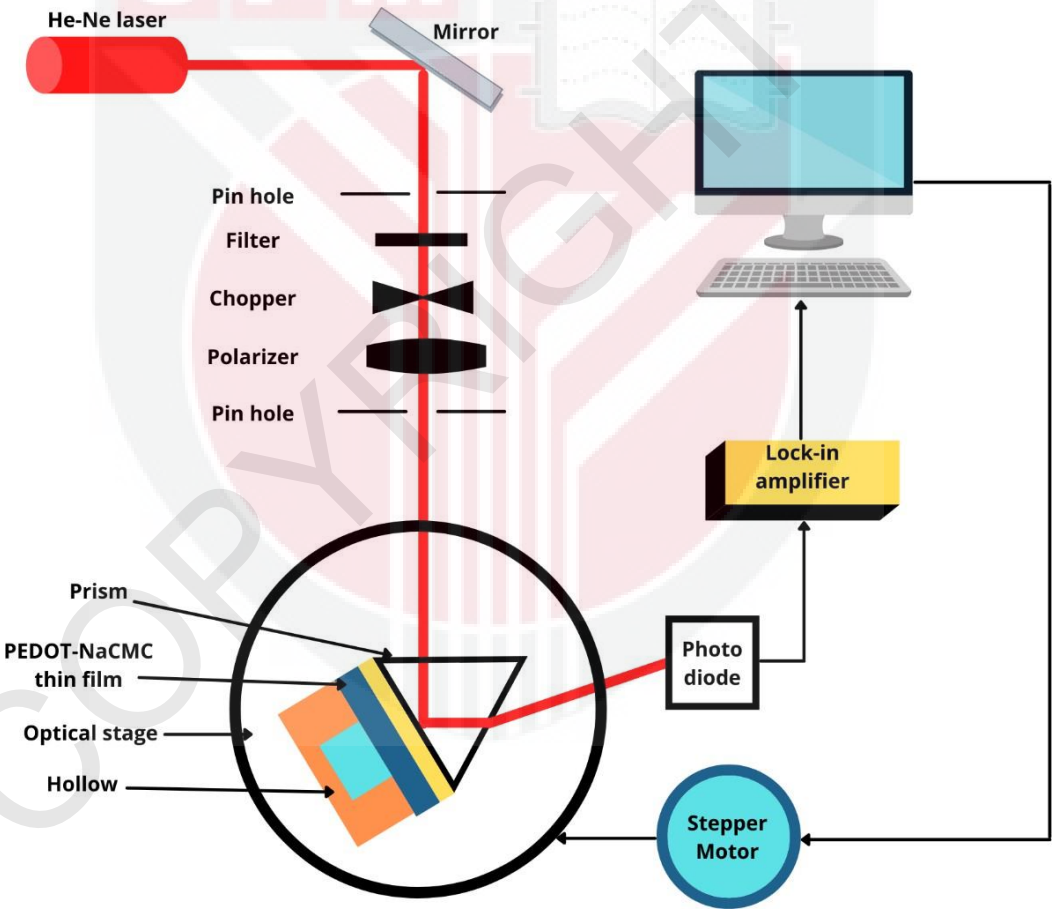

Figure 3.3: Experimental setup of SPR sensor.

CHAPTER 4

RESULTS AND DISCUSSION

4.1 Introduction

This chapter will discuss about the result obtained from the sample prepared by using methodology stated in in chapter 3 previously. Fourier transform infrared spectroscopy (FTIR) was used to identify the functional groups present in PEDOT, NaCMC, and PEDOT-NaCMC thin films. Meanwhile, the results of optical properties analysis of PEDOT, NaCMC and PEDOT-NaCMC thin films that include the absorption and optical band gap will be determined by using ultraviolet–visible spectroscopy (UV-Vis) and surface morphological of PEDOT-NaCMC thin film will be analyzed by using an atomic force microscope (AFM). Lastly, the surface plasmon resonance spectroscopy (SPR) was used to discover the sensing properties of a PEDOT-NaCMC thin film towards HQ solution.

4.2 Fourier Transform Infrared Spectroscopy

Fourier transform infrared spectroscopy (FTIR) spectrum was used to study the functional groups and chemical bonding exist in PEDOT, NaCMC and PEDOT-NaCMC. The FTIR is a plot of intensity of emission against transmitted frequencies. X-axis acts as wavenumber or frequencies and y-axis acts as transmitted frequencies and used as information on the presence of any functional groups in the compound.

The range 500 cm^{-1} to 4000 cm^{-1} of the IR spectrum of PEDOT, NaCMC and PEDOT-NaCMC thin films was shown in Figure 4.1. A broad absorption band at 3310 cm^{-1} was assigned to the stretching frequency of the –OH group from the PEDOT spectrum, corresponding to asymmetrical and symmetrical stretching vibrations of the hydroxyl group (–

OH), which could overlap the N–H stretching at the same region. The peak at 1633 cm^{-1} attributed to C=C stretching bond due to the quinoidal structure of PEDOT. Meanwhile, the characteristics bands seen at 1292 cm^{-1} and 1177 cm^{-1} could be attributed to stretching C–O–C bonds, as observed in a previous report by Zhang et al. in 2015, whereas PSS bands are seen at 1063 cm^{-1}, which belongs to the S=O vibration.

Next, from the spectrum of NaCMC shown in Figure 4.1, it can be observed that a broad absorption band at 3310 cm^{-1} which is due to the stretching frequency of the –OH group. The band present at 2923 cm^{-1} can be attributed to C–H stretching vibration while the presence of a strong absorption band at 1633 cm^{-1} represents O–H bending of absorbed water confirms the presence of COO^{-} group (Lin et al., 2013) .

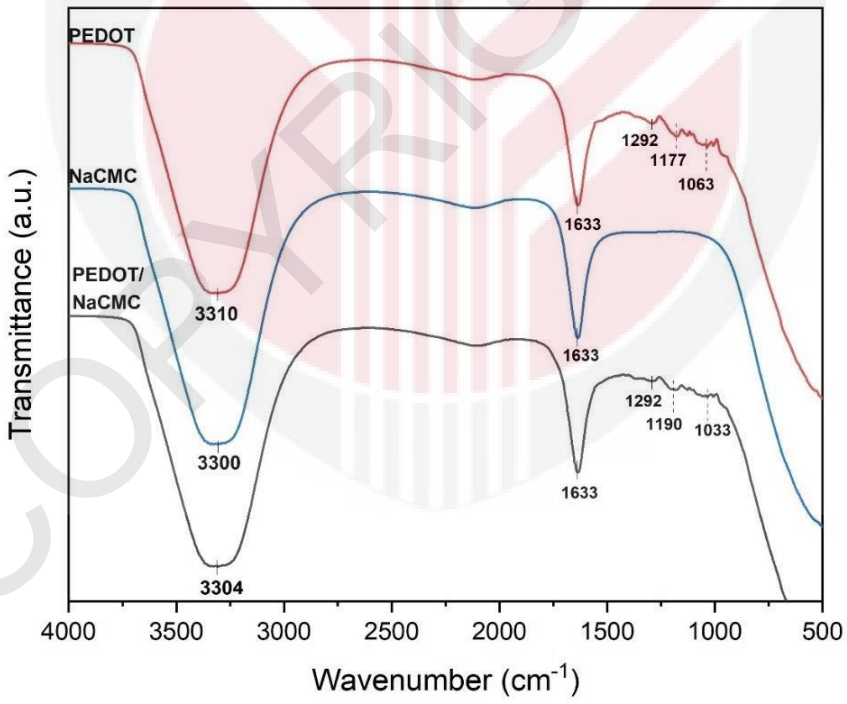

Figure 4.1: FTIR spectrum of PEDOT, NaCMC and PEDOT-NaCMC thin films.

The spectrum of PEDOT/NaCMC and PEDOT thin film has displayed a few common properties, which the absorption bands at 3304 cm^{-1} referred to as O–H stretching vibration. Besides the absorption band displayed at 1633 cm^{-1} assigned to O–H bending of absorbed water, there are also characteristic absorbance bands centred at 1292 cm^{-1} and 1190 cm^{-1}, which were produced by the C–O–C stretching vibration. Lastly, the S=O stretching bond is located at 1033 cm^{-1}.

The functional groups that exist match the spectra of the PEDOT-NaCMC thin film in a previous study by Zhang et al. (2015). The comparison of FTIR spectra of the PEDOT, NaCMC and PEDOT-NaCMC thin film proved the combination band of PEDOT and NaCMC. In general, the peak around 3200 cm^{-1} to 3400 cm^{-1} is assigned to the O–H group. Then, the O–H bending of absorbed water is located at around 1633 cm^{-1}. Meanwhile, ether and sulfonate groups only existed in PEDOT and PEDOT-NaCMC spectra. Table 4.1 shows the characteristics frequencies of PEDOT-NaCMC thin film.

Table 4.1: Characteristics frequencies of PEDOT-NaCMC thin film.

Wavenumber (cm^{-1})	Band Assignment
3304	–OH
1633	C=C
1292	C–O
1033	S=O

4.3 Ultraviolet–Visible Spectroscopy

4.3.1 Absorption Versus Wavelength

In context of optical analysis, the absorbance spectrum of the thin films was measured for wavelengths ranging from 220 nm to 900 nm using ultraviolet-visible spectrometer (UV-Vis). Figure 4.2 depicts the UV-Vis results of PEDOT, NaCMC, and PEDOT-NaCMC thin films, which show that the absorbance of each thin film varies. The maximum absorption peak for all three thin films can be found between 270 nm and 300 nm.

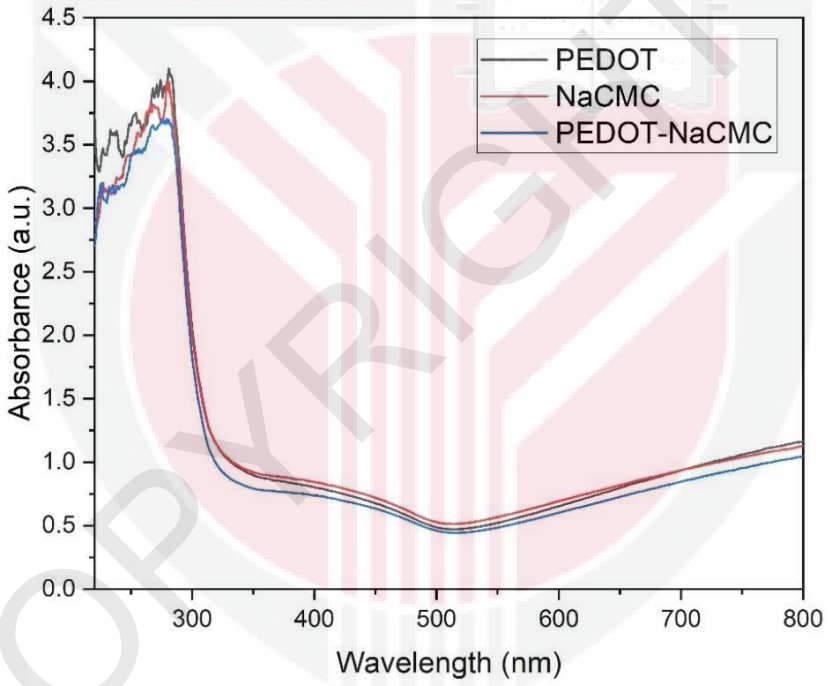

Figure 4.2: Absorbance spectrum of the PEDOT, NaCMC and PEDOT-NaCMC thin films.

The absorption spectra of PEDOT showed an absorbance value of approximately 4.10 at peak 280 nm, according to the graph, whereas PEDOT-NaCMC has an absorbance value of 3.70 at 274 nm and 278 nm, respectively. At 279 and 280 nm, NaCMC had an absorbance value of 3.99. The absorption peaks found at around 280 nm, which corresponds to the

n→π* transition of C=O, agree with previous studies that used PEDOT-based material, according to Figure 4.2. The absorbance peaks in the UV-Vis spectra of pristine PEDOT:PSS and its hybrid composites are 224 and 254 nm, which correspond to the aromatic ring of the PSS group (Seekaew et al., 2014).

4.3.2 Absorbance Coefficient

In this study, The Beer Lambert law theory was used to determine the absorbance, which according to theory that the concentration of substances in solution is directly proportional to absorbance. It also defines the relationship between absorbance (*A*) and transmittance (*T*). This law, however, only applies to monochromatic light. When monochromatic radiation passes through a homogeneous solution, the intensity of the emitted radiation is determined by the solution's thickness, *t*, and concentration.

The absorbance, *A* of samples depends on the ratio of intensities of the illumination falling on the detector in the absence I_o and the presence I_t of the sample.

$$A = log_{10} \frac{I_0}{I_t} \tag{4.1}$$

The transmittance, *T* of sample is given by:

$$T = \frac{I_0}{I_t} \tag{4.2}$$

Absorbance and transmittance are related, thus:

$$A = log_{10} T \tag{4.3}$$

The absorbance coefficient is another quantity that can be measured. It is a useful quantity to have when comparing samples of varying thickness. In this study, the atomic force microscopy was used to determine the thickness of each sample. The absorbance coefficient is represented as

$$\alpha = 2.303 \ \frac{A}{t} \tag{4.4}$$

In this equation, *t* is the sample thickness in unit meters (m), and the absorbance coefficient must be reported in units of m^{-1}. The absorbance coefficient in spectroscopy is directly derived from the illumination of the intensity of light at a specified wavelength that passes through a sample (transmitted light intensity), and I_o is the intensity of the light before it enters the sample (incident light intensity).

4.3.3 Energy Band Gap

Furthermore, the energy band gap of all three composites has been calculated, with the help of absorption spectra. In order to calculate the optical band gap energy using absorption spectra, the Tauc relation is used,

$$\alpha = \frac{k(hv - E_g)^{\frac{1}{2}}}{hv} \tag{4.5}$$

By rearrangement of the equation (4.5),

$$(\alpha hv)^2 = k(hv - E_g) \tag{4.6}$$

Where hv is photon energy, h is Plank's constant, α is absorption coefficient, E_g is the optical energy gap, k is constant, and $n = \frac{1}{2}$ for direct transitions. The value of the optical energy band gap, E_g, is given by the zero point of a fitted linear function of a plotted graph of $(\alpha hv)^2$ against hv (Jarosinkski et al., 2019). Figures 4.3, 4.4, and 4.5 show graphs of $(\alpha hv)^2$ versus hv for PEDOT thin film, NaCMC thin film, and PEDOT:NaCMC thin film, respectively.

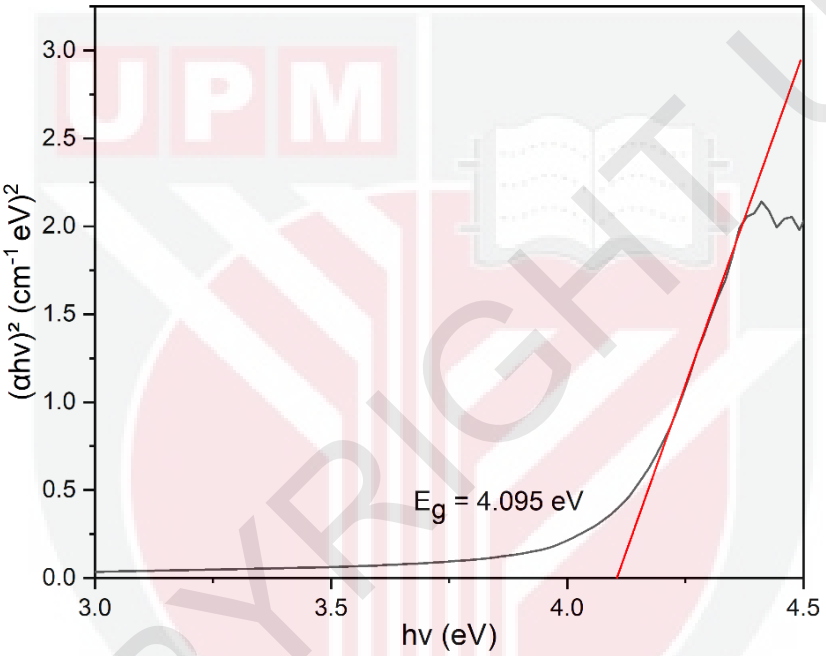

Figure 4.3: Optical band gap for PEDOT thin film.

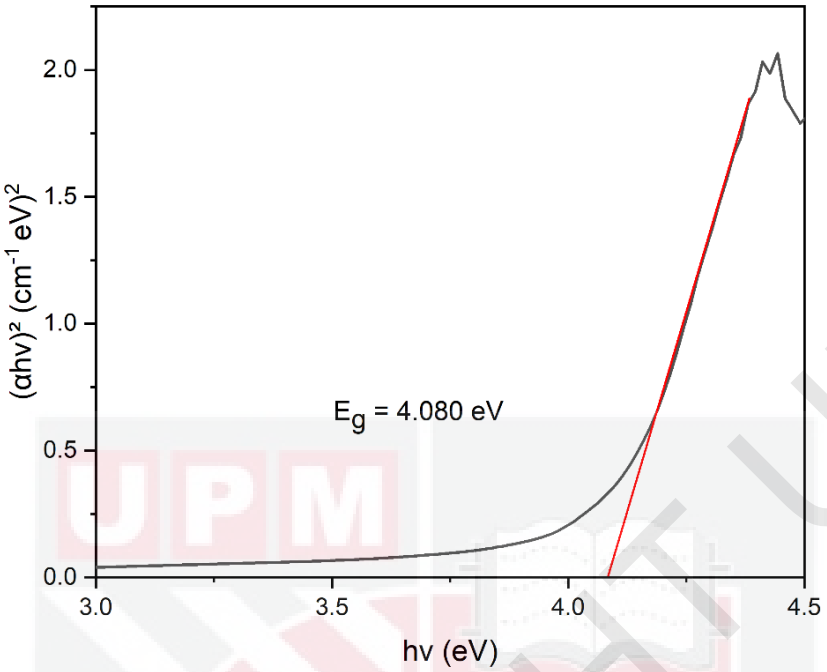

Figure 4.4: Optical band gap for NaCMC thin film.

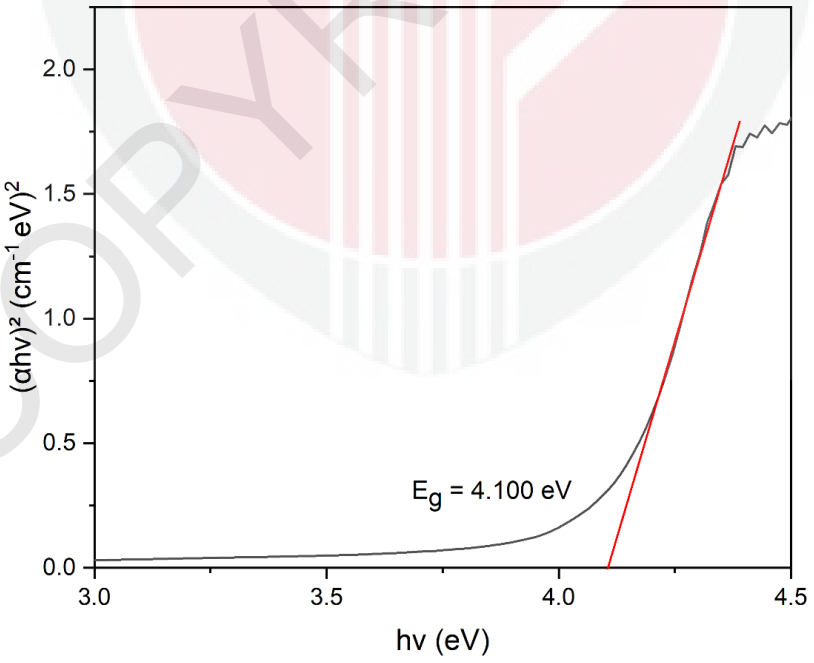

Figure 4.5: Optical band gap for PEDOT-NaCMC thin film.

As shown in the Figures 4.3-4.5, the intersection of the linear fitted line on the x-axis gives the value of the optical band gap. The plot of $(\alpha hv)^2$ versus hv PEDOT, NaCMC and PEDOT-NaCMC revealed a slight difference in the value of the energy band gap, E_g. The energy band gap for the PEDOT thin film was found to be 4.095 eV, and the band gap for the NaCMC thin film was found to be 4.080 eV when compared to the PEDOT. Meanwhile, the combination of PEDOT and NaCMC has the highest optical band gap of all three thin films, measured at 4.100 eV. This is probably due to decrease in size of particle when PEDOT is mixed with the NaCMC. As stated in research done by Singh et al. (2018), the optical band gap energy increases as particle size of the semiconductor nanomaterials decreases.

4.4 **Surface Plamon Resonance Analysis**

4.4.1 SPR Signal for Hydroquinone on Gold Single Layer

In this study, a preliminary test was carried on a gold single layer in contact with deionized water (DW), in which approximately 2 ml of DW was injected into the cell to ensure that it was in contact with the gold layer thin film. Then, it was left for a few minutes to ensure complete interaction between DW and the gold thin film.

According to the graph, the resonance angle for the SPR curve obtained is 53.2638°. The SPR experiment was then carried out with various concentrations of HQ in aqueous solution. Starting with the lowest concentration of 2 nM and progressing to the highest concentration of 10 nM, each concentration was injected one after the other into the cell attached to the gold layer thin film and was repeated three times to assess data accuracy. Figure 4.6 depicts the SPR curves of various concentrations of HQ in contact with a gold layer.

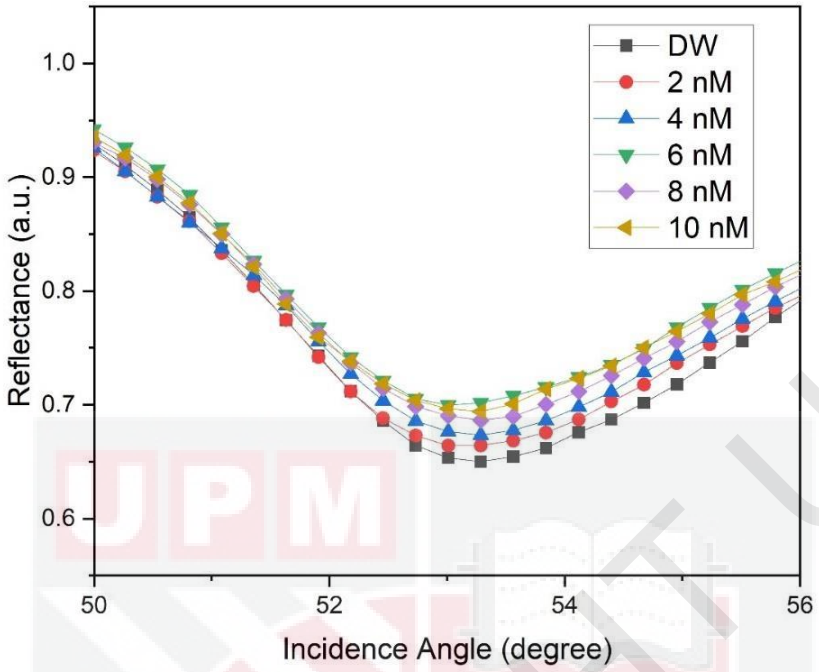

Figure 4.6: The reflectivity curves for HQ (0-10 nM) in contact with gold layer (DW represents 0 nM).

Figure 4.7 shows a comparison of the resonance angles for all different concentrations of HQ solution as well as DW. The results shows that the resonance angle was similar for all concentrations of HQ and deionized water. It demonstrates that the resonance angle of the sample in contact with the bare gold thin film did not change (Anas et al., 2019). The concentration of the samples used in this study was very low, implying that all of the samples have a similar refractive index. The sensor's gold surface is extremely sensitive to the refractive index of its surroundings (Zainuddin et al., 2018). Thus, similar refractive index of the samples caused in similar of resonance angle.

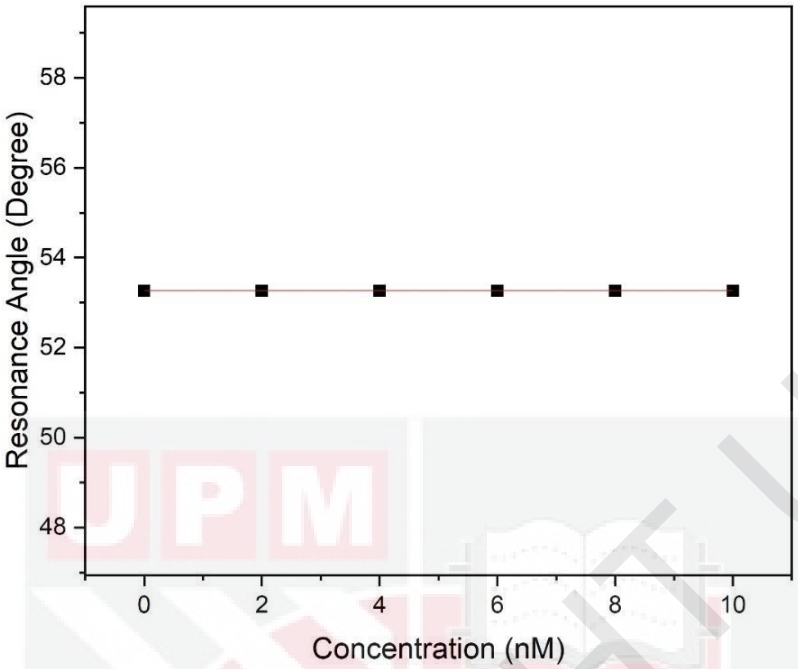

Figure 4.7: The resonance angle of gold surface in contact with different HQ concentration.

4.4.2 PEDOT-NaCMC SPR Signal for Hydroquinone on Gold Surface

The SPR experiment was then carried on by using a PEDOT-NaCMC composite on top of the gold layer thin film for hydroquinone (HQ) detection instead of the gold layer thin film. The HQ detection experiment's procedure was repeated, firstly with DW. The DW reflectivity curve was used as the reference value for comparing the curves for different concentrations of HQ. When PEDOT-NaCMC is used on a gold layer, the resonance angle shifts slightly to the right, as shown in Figure 4.8.

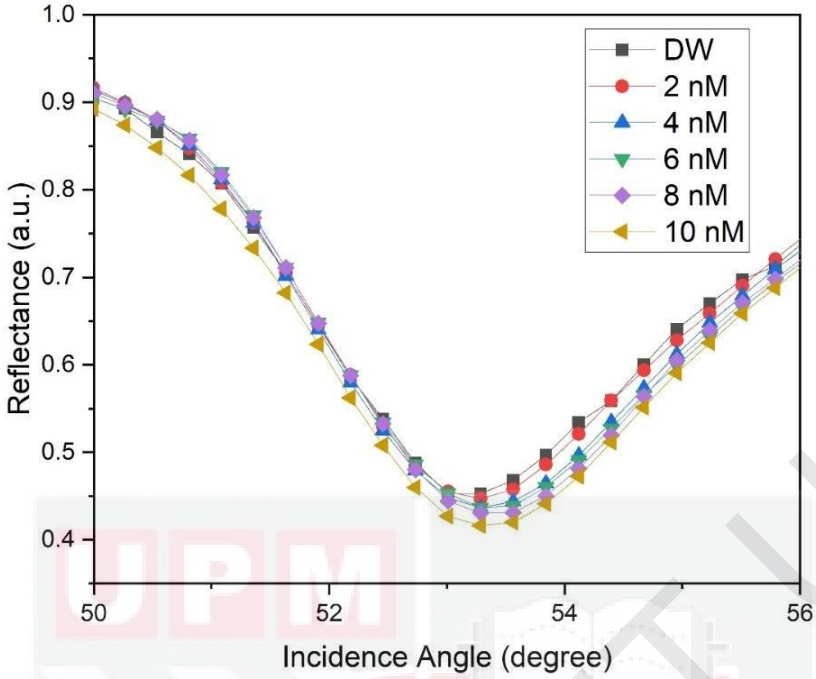

Figure 4.8: The reflectivity curves for PEDOT-NaCMC thin film in contact with different concentration of HQ solution ranged from 0-10 nM (DW represents 0 nM).

For DW, it can be seen that the resonance angle obtained was 53.2298°. The variation in resonance angle is caused by an increase in the sensing medium's or target's refractive index (Anas et al., 2020). The resonance angle shifted to the right when PEDOT-NaCMC was coated over the gold layer in this case. The resonance angles for different concentrations of HQ solutions exposed to the PEDOT-NaCMC thin film were 53.2900°, 53.3255°, 53.4090°, 53.4213°, and 53.3255° at concentrations of 2, 4, 6, 8, and 10 nM respectively. The shift to the left for 10 nM is most likely due to thin film degradation after several hours of exposure to HQ solution (Eddin et al., 2021).

4.4.3 Sensitivity of PEDOT-NaCMC Thin Film

The resonance angle shift (Δθ) is introduced as a parameter to calculate the sensor sensitivity (Ramdzan et al., 2021). In this work, (Δθ) was used to investigate the sensitivity of the PEDOT-NaCMC thin film. The value of Δθ was determined using the difference between the resonance angle of HQ concentration and DW as a reference. Tables 4.2 and 4.3 show the resonance angle and shift of resonance angle for HQ concentrations ranging from 2 nM to 10 nM in-contact to gold layer thin film with and without PEDOT-NaCMC deposition respectively. Meanwhile, Figures 4.9 show a graph of the gold thin film with and without PEDOT-NaCMC deposition against HQ concentrations to discuss the sensor's sensitivity. These plots clearly show that the presence of PEDOT-NaCMC composites increases the sensitivity for HQ detection.

Table 4.2: The SPR resonance angle and shift of resonance angle for different concentration of HQ solution in contact with gold layer thin film (0 nM represents deionized water).

Concentration of HQ (nM)	Resonance Angle, θ (degree)	Shift of Resonance Angle, Δθ (degree)
0	53.2638	0
2	53.2638	0
4	53.2638	0
6	53.2638	0
8	53.2638	0
10	53.2638	0

Table 4.3: The SPR resonance angle and shift of resonance angle for different concentration of HQ solution in contact with PEDOT-NaCMC thin film (0 nM represents deionized water).

Concentration of HQ (nM)	Resonance Angle, θ (degree)	Shift of Resonance Angle, Δθ (degree)
0	53.2298	0
2	53.2900	0.0602
4	53.3255	0.0957
6	53.4090	0.1792
8	53.4213	0.1915
10	53.3255	0.0957

According to Table 4.2 and Figure 4.9, the resonance angle for HQ concentrations does not change when it comes into contact with the gold layer film. Meanwhile, the deposition of PEDOT-NaCMC on the gold layer increased the resonance angle when exposed to HQ up to 8 nM and then decreased due to degradation of in the thin film after several hours of exposure to HQ solution (Eddin et al., 2021). The linear fit for the PEDOT-NaCMC thin film shows a good response up to 8 nM HQ concentration with linear regression coefficients R^2 of 0.953 and the relationship between the SPR angle shift ($\Delta\theta_{SPR}$) and HQ concentrations was governed by the Equation $\Delta\theta_{SPR}$= 0.0251[HQ] + 0.00275. The gradient of the linear regression plot can be defined as the sensitivity of the active layer towards the HQ. As a result, the linear regression plot yields a gradient of 0.0251° nM^{-1}. The sensor's high sensitivity was achieved by achieving a large shift in resonance angle with a small change in parameters like concentration, refractive index, and thickness. Changes in concentration cause the resonance angle to shift in this case (Anas et al., 2020).

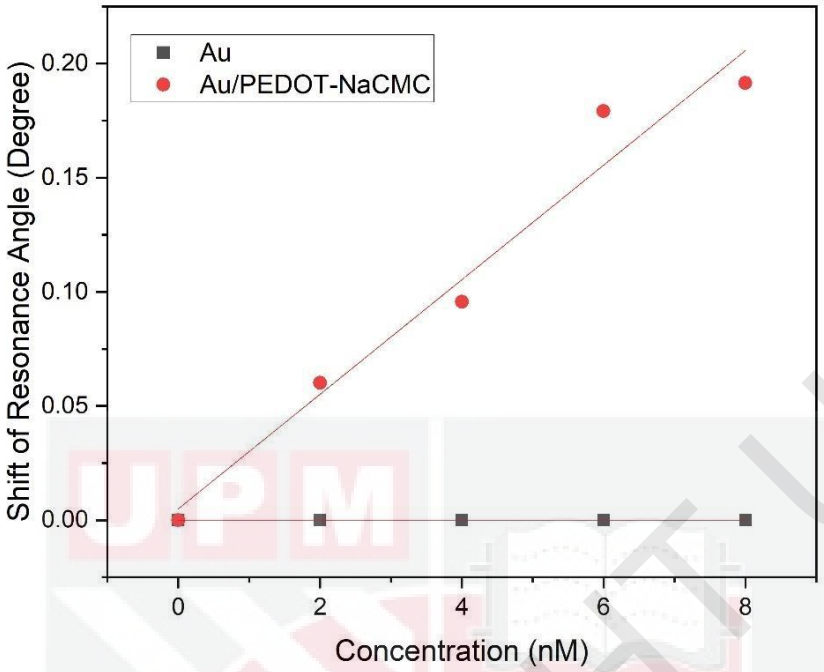

Figure 4.9: SPR angle shift against HQ concentration for gold (Au) and Au/PEDOT-NaCMC thin film.

4.3 Atomic Force Microscope

The morphology characteristics of the proposed thin films, PEDOT-NaCMC, were investigated using atomic force microscopy (AFM) in tapping mode. In this study, a scan size of 1 µm × 1 µm was selected to obtain the most precise image. The root mean square (RMS) roughness obtained from AFM images indicates the relative roughness and the standard deviation of the surface height (Ramdzan et al., 2021). Figure 4.10 shows two-dimensional (2D) and three-dimensional (3D) AFM images of the PEDOT-NaCMC thin film before and after contact with HQ solution.

(a)

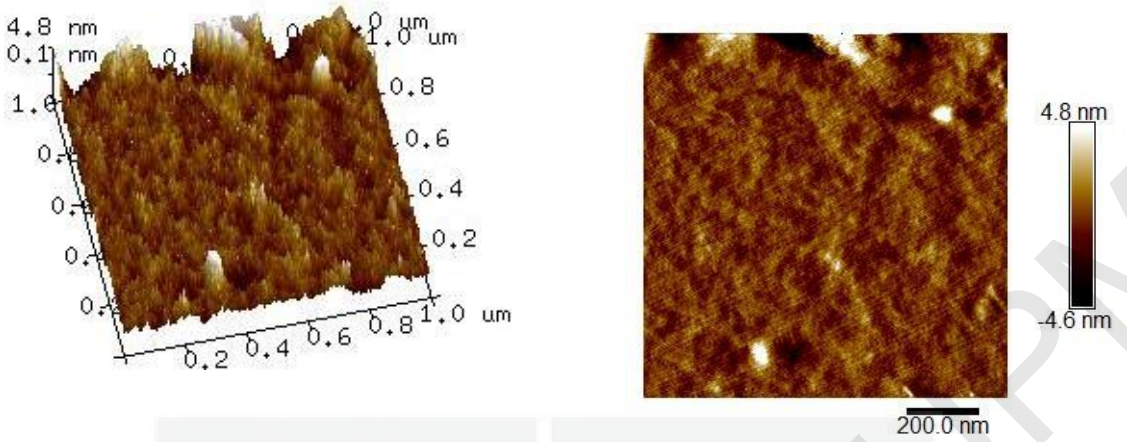

(b)

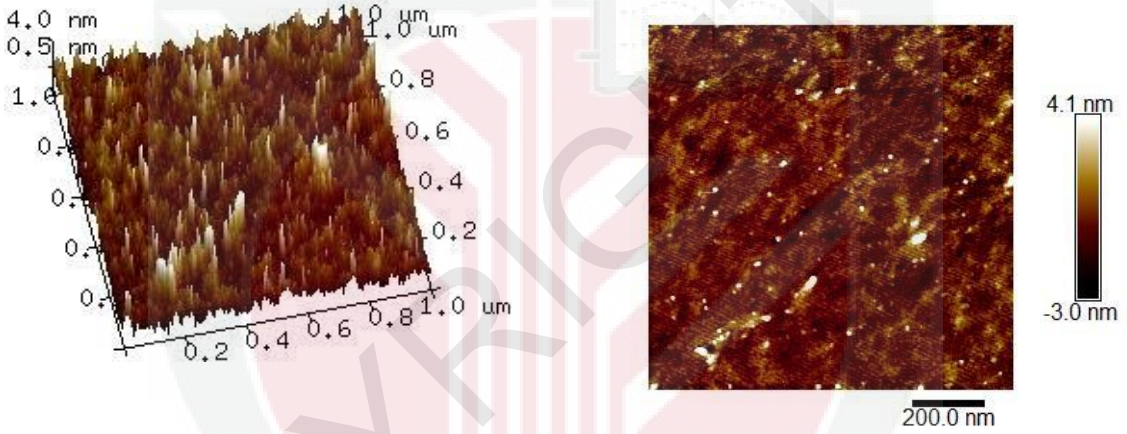

Figure 4.10: AFM image of PEDOT-NaCMC thin film (a) before and (b) after in contact with HQ solution.

The images show that the surface of the thin films was optimally covered with composite material. Based on the morphologies of the PEDOT-NaCMC thin film, it can be seen that PEDOT-NaCMC has a relatively smooth morphological characteristic with granular structure, with the magnitude of the surface roughness (Rq) of PEDOT-NaCMC before contact with HQ solution being 1.60 nm and decreasing to 0.91 nm after the HQ solution was added to the composite thin film. In addition, as shown in Fig. 4.10(b), there were multiple sharp peaks and microneedle-like structures visible in 3D view images (Daniyal et al., 2018). This result is most likely due to HQ adsorption by PEDOT-NaCMC, which results in a smoother surface

than the surface before in-contact with HQ (Anas et al., 2020). The adsorption of HQ was undoubtedly facilitated by the combining PEDOT with NaCMC, which increased the shift of the resonance angle for the HQ. The appearance of numerous sharp peaks in the 3D image indicated that the interaction of HQ and the PEDOT-NaCMC altered the surface morphology (Ramdzan et al., 2021).

CHAPTER 5

CONCLUSION

5.1 CONCLUSION

In this study, the thin films of PEDOT, NaCMC and PEDOT-NaCMC were characterized by using the FTIR spectroscopy while the surface morphology and surface roughness of the PEDOT-NaCMC thin films before and after in-contact with HQ solution were observed by using AFM. Meanwhile, the optical properties of the thin films were successfully studied using the UV-Visible spectroscopy.

The results from FTIR spectra show almost the same peak for all three solutions. The peak for found for PEDOT-NaCMC absorption bands at 3304 cm^{-1} and 1633 cm^{-1} assigned to O–H stretching vibration and O–H bending of absorbed water respectively. There were also absorbance bands displayed at peak 1292 cm^{-1} and 1190 cm^{-1} which were produced by the C–O–C stretching vibration. Meanwhile, the absorbance peaks located at 1033 cm^{-1} referred to S=O stretching bond.

The surface morphology characterization results by using AFM displayed a result of PEDOT-NaCMC before and after in-contact with the HQ solutions. From the results obtained, it can be observed that before in-contact with HQ, PEDOT-NaCMC has a fairly smooth of granular and after being exposed to the HQ solution, the surface roughness of the thin film decreased.

Next, in order to study the absorbance values and energy band gap of the three types of thin films, the UV-Visible spectrometer was used. The PEDOT-NaCMC thin film has the lowest absorbance value of 3.70 at 274 nm and 278 nm respectively compared to the PEDOT and NaCMC thin film. Meanwhile, the optical band gap for PEDOT, NaCMC and PEDOT-NaCMC were 4.095 eV, 4.080 eV and 4.100 eV respectively.

Lastly, the sensing properties of the PEDOT-NaCMC thin film has been investigated using surface plasmon resonance spectroscopy where it can be identified that thin film coated with PEDOT-NaCMC was a suitable thin film to be used for the SPR experiment. The result displayed that the thin film produced a positive response towards HQ solutions of different concentration due to the interaction formed between HQ and PEDOT-NaCMC. Based on the comparison of resonance angle shift for both gold thin films and gold coated with PEDOT-NaCMC thin film, there were apparent right shift of angle for PEDOT-NaCMC thin film as the concentration of HQ solution increased. The sensitivity gained from the result was 0.0251° nM^{-1} with the limit of detection of HQ solution gained was as low as 2 nM.

To summarize, the results obtained from the study shows that the PEDOT-NaCMC composites thin film shows significant sensing properties and has a great potential in detecting of HQ in various concentration. This also indicates the versatility of sensing ability of the composites which could contributes important application in the future of biosensing field.

5.2 FUTURE WORK RECOMMENDATION

To further improve this work, the morphology and particle size distributions as well as the optical properties of the PEDOT-NaCMC can be further studied by using another structural analysis method such as high-resolution transmission electron microscopy (HRTEM) (HRTEM), field emission scanning electron microscopy (FESEM) and Photoluminescence. Moreover, it would be interesting to study the sensing properties of PEDOT-NaCMC thin film towards other type of phenol such as Resorcinol. Last but not least, a future study investigating other material that is suitable in improving the sensitivity and selectivity of the sensor would be good to be done in future.

REFERENCES

Abdi, M. M., Mahmood, W., Yunus, M., Reayi, M., & Bahrami, A. (2012). Plasmonic conducting polymers for heavy metal sensing. *Plasmonics-Principles and Applications*. *16*, 15–21. https://doi.org/10.5772/51337

Akar, E., & Altınıs, A. (2012). Preparation of pH- and ionic-strength responsive biodegradable fumaric acid crosslinked carboxymethyl cellulose. *90*, 1634–1641. https://doi.org/10.1016/j.carbpol.2012.07.043

Anas, N. A. A., Fen, Y. W., Omar, N. A. S., Ramdzan, N. S. M., Daniyal, W. M. E. M. M., Saleviter, S., & Zainudin, A. A. (2019). Optical properties of chitosan/hydroxyl-functionalized graphene quantum dots thin film for potential optical detection of ferric (III) ion. *Optics and Laser Technology*, *120*, 105724. https://doi.org/10.1016/j.optlastec.2019.105724

Anas, N. A. A., Fen, Y. W., Yusof, N. A., Omar, N. A. S., Mohd Daniyal, W. M. E. M., & Ramdzan, N. S. M. (2020). Highly sensitive surface plasmon resonance optical detection of ferric ion using CTAB/hydroxylated graphene quantum dots thin film. *Journal of Applied Physics*, *128*(8), 83105. https://doi.org/10.1063/5.0018106

Badry, R., El, S., Hanan, K., Nadra, E., & Medhat, N. (2021). Optical, conductivity and dielectric properties of plasticized solid polymer electrolytes based on blends of sodium carboxymethyl cellulose and polyethylene oxide. *Optical and Quantum Electronics*, *53*(1), 1–15. https://doi.org/10.1007/s11082-020-02649-2

Barbucci, R., Magnani, A., & Consumi, M. (2000). Swelling behavior of carboxymethylcellulose hydrogels in relation to cross-linking, pH, and charge density. *Macromolecules*, *33*(20), 7475–7480. https://doi.org/10.1021/ma0007029

Chao, Y., Zhang, X., Liu, L., & Tian, L. (2015). Determination of hydroquinone by flow injection chemiluminescence and using magnetic surface molecularly imprinted particles. *Michromica Acta, 182*, 943–948. https://doi.org/10.1007/s00604-014-1415-2

Chen, J., Gao, Y., Hu, X., Xu, Y., & Lu, X. (2019). Detection of hydroquinone with a novel fluorescence probe based on the enzymatic reaction of graphite phase carbon nitride quantum dots. *Talanta*, *194*, 493–500. https://doi.org/10.1016/j.talanta.2018.09.111

Chen, T., Xu, J., Arsalan, M., Sheng, Q., Zheng, J., Cao, W., & Yue, T. (2019). Controlled synthesis of Au@Pd core-shell nanocomposites and their application for electrochemical sensing of hydroquinone. *Talanta, 198,* 78–85. https://doi.org/10.1016/j.talanta.2019.01.094

Daniyal, W. M. E. M. M., Fen, Y. W., Abdullah, J., Sadrolhosseini, A. R., Saleviter, S., & Omar, N. A. S. (2018). Exploration of surface plasmon resonance for sensing copper ion based on nanocrystalline cellulose-modified thin film. *Optics Express, 26*(26), 34880. https://doi.org/10.1364/oe.26.034880

Fauzi, N. I. M., Fen, Y. W., Omar, N. A. S., Saleviter, S., Daniyal, W. M. E. M. M., Hashim, H. S., & Nasrullah, M. (2020). Nanostructured chitosan/maghemite composites thin film for potential optical detection of mercury ion by surface plasmon resonance investigation. *Polymers*, *12*(7), 1–13. https://doi.org/10.3390/polym12071497

Fu, J., Pang, Z., Yang, J., Huang, F., Cai, Y., & Wei, Q. (2015). Fabrication of polyaniline/ carboxymethyl cellulose/cellulose nanofibrous mats and their biosensing application. *Applied Surface Science*, *349*, 35-42. https://doi.org/10.1016/j.apsusc.2015.04.215

Gad, S. C., & Pham, T. (2014). Hydroquinone. *Encyclopedia of Toxicology: Third Edition*, *2*, 979–981. https://doi.org/10.1016/B978-0-12-386454-3.00855-1

Gueye, M. N., Carella, A., Faure-Vincent, J., Demadrille, R., & Simonato, J. P. (2020). Progress in understanding structure and transport properties of PEDOT-based materials: A critical review. *Progress in Materials Science*, *108*, 100616. https://doi.org/10.1016/j.pmatsci.2019.100616

Hashim, H. S., Fen, Y. W., Omar, N. A. S., Daniyal, W. M. E. M. M., Saleviter, S., & Abdullah, J. (2020). Structural, optical and potential sensing properties of tyrosinase immobilized graphene oxide thin film on gold surface. *Optik*, *212*, 164786. https://doi.org/10.1016/j.ijleo.2020.164786

Hashim, H. S., Fen, Y. W., Sheh Omar, N. A., Abdullah, J., Daniyal, W. M. E. M. M., & Saleviter, S. (2020). Detection of phenol by incorporation of gold modified-enzyme based graphene oxide thin film with surface plasmon resonance technique. *Optics Express*, *28*(7), 9738. https://doi.org/10.1364/oe.387027

Hebbar, V., Bhajantri, R. F., & Naik, J. (2017). Influence of graphene nanoparticles on optical and dielectric properties of PVA-PEDOT:PSS blend composite. *AIP Conference Proceedings*, *1832*, 050046. https://doi.org/10.1063/1.4980279

Hryniewicz, B. M., Orth, E. S., & Vidotti, M. (2018). Enzymeless PEDOT-based electrochemical sensor for the detection of nitrophenols and organophosphates. *Sensors and Actuators, B: Chemical*, *257*, 570–578. https://doi.org/10.1016/j.snb.2017.10.162

Huang, H., Xu, M., Gao, Y., Wang, G., & Su, X. (2011). Water-soluble fluorescent conjugated polymer-enzyme hybrid system for the determination of both hydroquinone and hydrogen peroxide. *Talanta*, *86*(1), 164–169. https://doi.org/10.1016/j.talanta.2011.08.053

Kamal Eddin, F. B., Fen, Y. W., Omar, N. A. S., Liew, J. Y. C., & Daniyal, W. M. E. M. M. (2021). Femtomolar detection of dopamine using surface plasmon resonance sensor based on chitosan/graphene quantum dots thin film. *Spectrochimica Acta-Part A: Molecular and*

Biomolecular Spectroscopy, *263*, 120202. https://doi.org/10.1016/j.saa.2021.120202

Kundu, J., Mohapatra, R., & Kundu, S. C. (2011). Silk fibroin/sodium carboxymethyl cellulose blended films for biotechnological applications. *22*(4), 519–539. https://doi.org/10.1163/092050610X487864

Li, Z., Ni, P., Dai, H., Li, Z., Sun, Y., Hu, J., Jiang, S., & Wang, Y. (2015). Carbon dots based fluorescent sensor for sensitive determination of hydroquinone. *Talanta*, *144*(2), 258–262. https://doi.org/10.1016/j.talanta.2015.06.014

Lin, X., Li, Y., Chen, Z., Zhang, C., Luo, X., Du, X., & Huang, Y. (2013). Synthesis , characterization and electrospinning of new thermoplastic carboxymethyl cellulose (TCMC). *Chemical Engineering Journal*, *215*, 709–720. https://doi.org/10.1016/j.cej.2012.10.089

Liu, Yingnan, Wang, Q., Guo, S., Jia, P., Shui, Y., Yao, S., Huang, C., Zhang, M., & Wang, L. (2018). Highly selective and sensitive fluorescence detection of hydroquinone using novel silicon quantum dots. *Sensors and Actuators, B: Chemical*, *275*, 415–421. https://doi.org/10.1016/j.snb.2018.08.073

Liu, Yuxia. (2020). Synthesis of iron (III) tetracarboxyl-phthalocyanine sensitized nano TiO_2 composite as photoelectrochemical hydroquinone sensor. *International Journal of Electrochemical Science*, *15*, 7575–7584. https://doi.org/10.20964/2020.08.29

Luna-Martínez, J. F., Hernández-Uresti, D. B., Reyes-Melo, M. E., Guerrero-Salazar, C. A., González-González, V. A., & Sepúlveda-Guzmán, S. (2011). Synthesis and optical characterization of ZnS-sodium carboxymethyl cellulose nanocomposite films. *Carbohydrate Polymers*, *84*(1), 566–570. https://doi.org/10.1016/j.carbpol.2010.12.021

Mo, G., He, X., Zhou, C., Ya, D., Feng, J., Yu, C., & Deng, B. (2018). Sensitive detection of hydroquinone based on electrochemiluminescence energy transfer between the exited ZnSe quantum dots and benzoquinone. *Sensors & Actuators: B. Chemical, 20,* 884. https://doi.org/10.1016/j.snb.2018.03.187

Mohanadas, D., Tukimin, N., & Sulaiman, Y. (2019). Simultaneous electrochemical detection of hydroquinone and catechol using poly (3 , 4-ethylenedioxythiophene)/ reduced graphene oxide / manganese dioxide. *Synthetic Metals*, *252*, 76–81. https://doi.org/10.1016/j.synthmet.2019.04.014

Mohd, W., Mustaqim, E., Daniyal, M., Fen, Y. W., Illya, N., Fauzi, M., Hashim, H. S., Ramdzan, N. S., Alia, N., & Omar, S. (2020). Recent advances in surface plasmon resonance optical sensors for potential application in environmental monitoring. *Sensors and materials*, *32*(12), 4191–4200. http://dx.doi.org/10.18494/SAM.2020.3204

Pasha, A., & Khasim, S. (2018). Highly sensitive ethylene glycol-doped PEDOT – PSS organic thin films for LPG sensing. *RSC Advances*, *8*, 18074–18083. https://doi.org/10.1039/C8RA01061G

Pattnaik, P. (2005). Surface plasmon resonance: Applications in understanding receptor-ligand interaction. *Applied Biochemistry and Biotechnology*, *126*(2), 79–92. https://doi.org/10.1385/abab:126:2:079

Prema, P., Thangapandiyan, S., & Immanuel, G. (2016). CMC stabilized nano silver synthesis, characterization and its antibacterial and synergistic effect with broad spectrum antibiotics. *Carbohydrate Polymers, 158,* 141–148. https://doi.org/10.1016/j.carbpol.2016.11.083

Qian, J., Yang, Z., Cui, H., An, K., Ren, C., Liu, Q., & Wang, K. (2020). Fabricating a signal-off photoelectrochemical sensor based on $BiPO_4$-graphene quantum dots nanocomposites

for sensitive and selective detection of hydroquinone. *Journal of Electroanalytical Chemistry*, *868*, 114177. https://doi.org/10.1016/j.jelechem.2020.114177

Ramdzan, N. S. M., Fen, Y. W., Liew, J. Y. C., Omar, N. A. S., Anas, N. A. A., Daniyal, W. M. E. M. M., & Fauzi, N. I. M. (2021). Exploration on structural and optical properties of nanocrystalline cellulose/poly(3,4-ethylenedioxythiophene) thin film for potential plasmonic sensing application. *Photonics*, *8*(10), 419–433. https://doi.org/10.3390/photonics8100419

Ramdzan, N. S. M., Fen, Y. W., Omar, N. A. S., Anas, N. A. A., Liew, J. Y. C., Daniyal, W. M. E. M. M., & Hashim, H. S. (2021). Detection of mercury ion using surface plasmon resonance spectroscopy based on nanocrystalline cellulose/poly(3,4-ethylenedioxythiophene) thin film. *Measurement*, *182*, 109728. https://doi.org/10.1016/j.measurement.2021.109728

Rosddi, N. N. M., Fen, Y. W., Omar, N. A. S., Anas, N. A. A., Hashim, H. S., Ramdzan, N. S. M., Fauzi, N. I. M., Anuar, M. F., & Daniyal, W. M. E. M. M. (2021). Glucose detection by gold modified carboxyl-functionalized graphene quantum dots-based surface plasmon resonance. *Optik*, *239*, 166779. https://doi.org/10.1016/j.ijleo.2021.166779

Seekaew, Y., Lokavee, S., Phokharatkul, D., Wisitsoraat, A., Kerdcharoen, T., & Wongchoosuk, C. (2014). Low-cost and flexible printed graphene-PEDOT:PSS gas sensor for ammonia detection. *Organic Electronics*, *15*(11), 2971–2981. https://doi.org/10.1016/j.orgel.2014.08.044

Si, W., Lei, W., Han, Z., Hao, Q., Zhang, Y., & Xia, M. (2014). Selective sensing of catechol and hydroquinone based on composites. *Sensors & Actuators: B. Chemical*, *199*, 154–160. https://doi.org/10.1016/j.snb.2014.03.096

Singh, M., Goyal, M., & Devlal, K. (2018). Size and shape effects on the band gap of semiconductor compound nanomaterials. *Journal of Taibah University for Science*, *12*(4), 470–475. https://doi.org/10.1080/16583655.2018.1473946

Song, K. (2017). Interphase characterization in rubber nanocomposites. *Progress in Rubber Nanocomposites*, *2*, 115-152. https://doi.org/10.1016/B978-0-08-100409-8.00004-8

Tian, F., Li, H., Li, M., Li, C., Lei, Y., & Yang, B. (2017). Synthesis of one-dimensional poly(3,4-ethylenedioxythiophene)-graphene composites for the simultaneous detection of hydroquinone, catechol, resorcinol, and nitrite. *Synthetic Metals*, *226*(2), 148–156. https://doi.org/10.1016/j.synthmet.2017.02.016

Verma, R., & Gupta, B. D. (2015). Detection of heavy metal ions in contaminated water by surface plasmon resonance based optical fibre sensor using conducting polymer and chitosan. *Food Chemistry*, *166*, 568–575. https://doi.org/10.1016/j.foodchem.2014.06.045

Wang, H., Chen, D., Wei, Y., Yu, L., Zhang, P., & Zhao, J. (2011). A localized surface plasmon resonance light scattering-based sensing of hydroquinone via the formed silver nanoparticles in system. *Spectrochimica Acta-Part A: Molecular and Biomolecular Spectroscopy*, *79*(5), 2012–2016. https://doi.org/10.1016/j.saa.2011.04.025

Wang, P., Huang, D., Guo, W., & Di, J. (2017). Photoelectrochemical sensing for hydroquinone based on gold nanoparticle-modified indium tin oxide glass electrode. *Journal of Solid State Chemistry*, *22*(2), 123–128. https://doi.org/10.1007/s10008-017-3730-0

Wang, Y., Liu, Y., & Yang, M. (2020). Molecularly imprinted electrochemiluminescence sensor for sensitive and selective detection of hydroquinone molecularly imprinted electrochemiluminescence sensor for sensitive and selective detection of hydroquinone.

Chemistry Letters, *49*(7), 855-858. https://doi.org/10.1246/cl.190878

Wen, Y., & Xu, J. (2017). Scientific importance of water-processable pedot–pss and preparation, challenge and new application in sensors of its film electrode: A Review. *Journal of Polymer Science, Part A: Polymer Chemistry*, *55*(7), 1121–1150. https://doi.org/10.1002/pola.28482

Yao, Y., Wen, Y., & Xu, J. (2014). Composite electrode as sensing platform for the simultaneous electrochemical determination of dihydroxybenzene isomers. *Monatshefte fuer Chemie/Chemical Monthly*, *145*(1), 137–146. https://doi.org/10.1007/s00706-013-1003-x

Zhang, G., Tang, Y., Sun, Y., & Yu, H. (2016). A chemiluminescence method to detect hydroquinone with water-soluble sulphonato-(salen) manganese (III) complex as catalyst. *Luminescence:The Journal of Biological and Chemical Luminescence*, *31*(1), 195–201. https://doi.org/10.1002/bio.2945

Zhang, Hua, Li, H., Li, J., Sun, H., Zhou, L., & Wang, R. (2019). A novel photoelectrochemical sensor based on Gr-SiNWs-Si/Pt electrode for sensing of hydroquinone. *International Journal of Electrochemical Science*, *14*, 1794-1808. https://doi.org/10.20964/2019.02.33

Zhang, Hui, Xu, J., Wen, Y., Wang, Z., & Zhang, J. (2015). Conducting poly(3,4-ethylenedioxythiophene):poly(styrene-sulfonate) film electrode with superior long-term electrode stability in water and synergistically enhanced electrocatalytic ability for application in electrochemical sensors. *Synthetic Metals*, *204*, 39–47. https://doi.org/10.1016/j.synthmet.2015.03.010

Zhao, X., Lyu, H., Yao, X., Xu, C., & Liu, Q. (2020). Hydroquinone colorimetric sensing based on platinum deposited on CdS nanorods as peroxidase mimics. *Microchimica Acta*, *187*(10), 587. https://doi.org/10.1007/s00604-020-04451-z